

CPOD2022 - Workshop on Critical Point and Onset of Deconfinement

Light Hypernuclei Measurements in Au+Au Collisions from STAR

Xiujun Li

(for the STAR collaboration)

University of Science and Technology of China



Supported in part by the



U.S. DEPARTMENT OF
ENERGY

Office of
Science

Outline

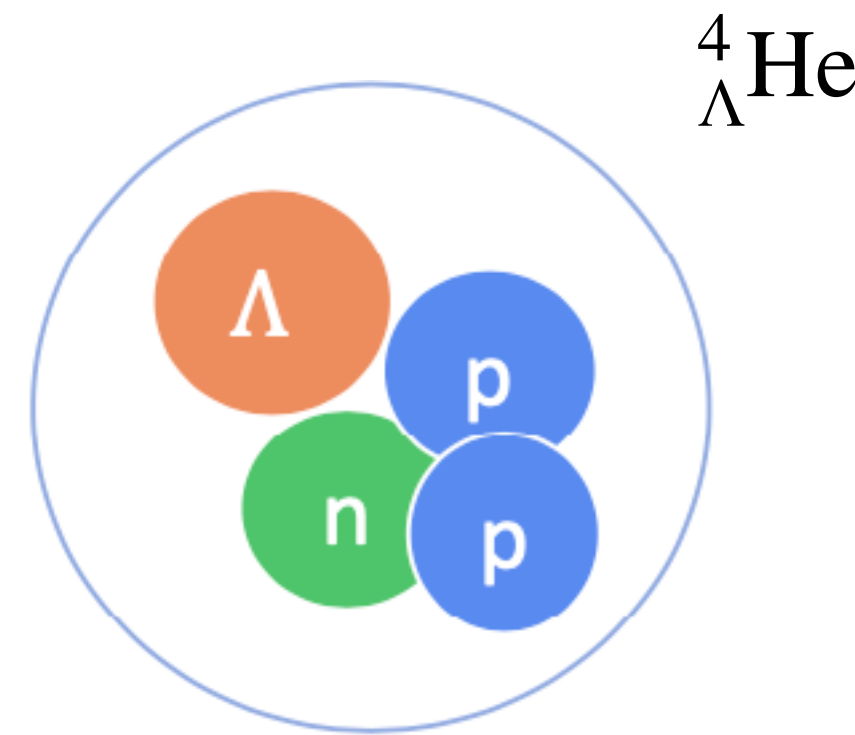
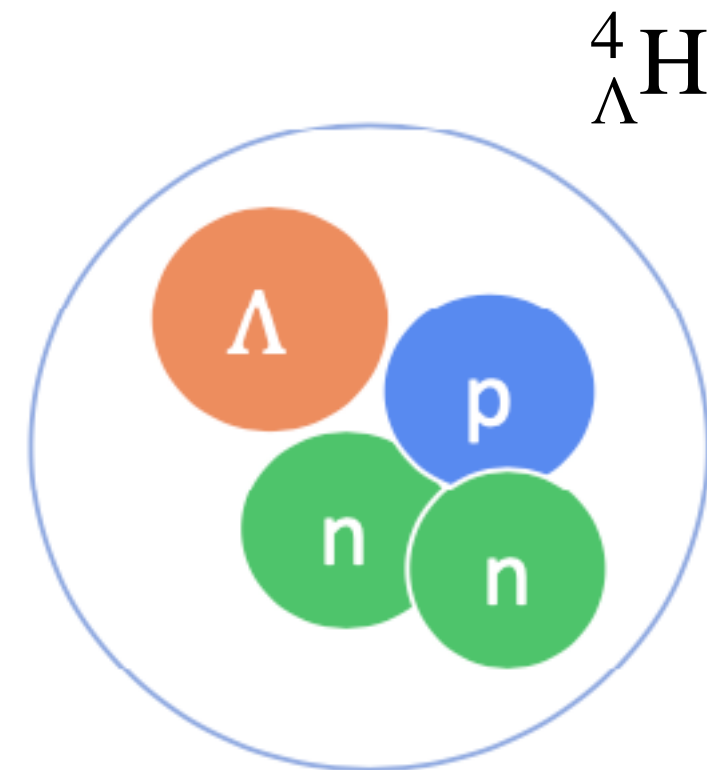
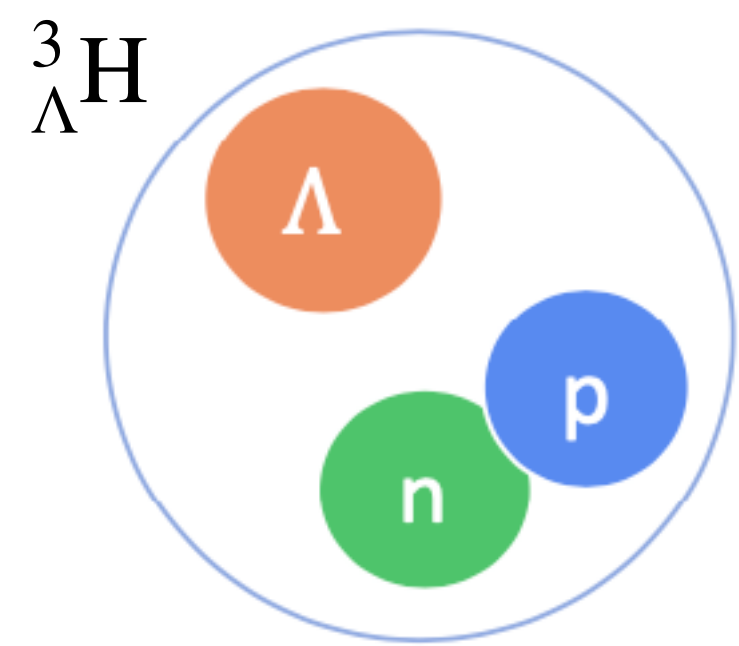


- Introduction
- Hypernuclei measurements in STAR BES-II
 - Internal structure
 - Branching ratios, lifetimes
 - Production mechanism
 - Yields, particle ratios, directed flow
- Summary and outlook

Introduction: what and why

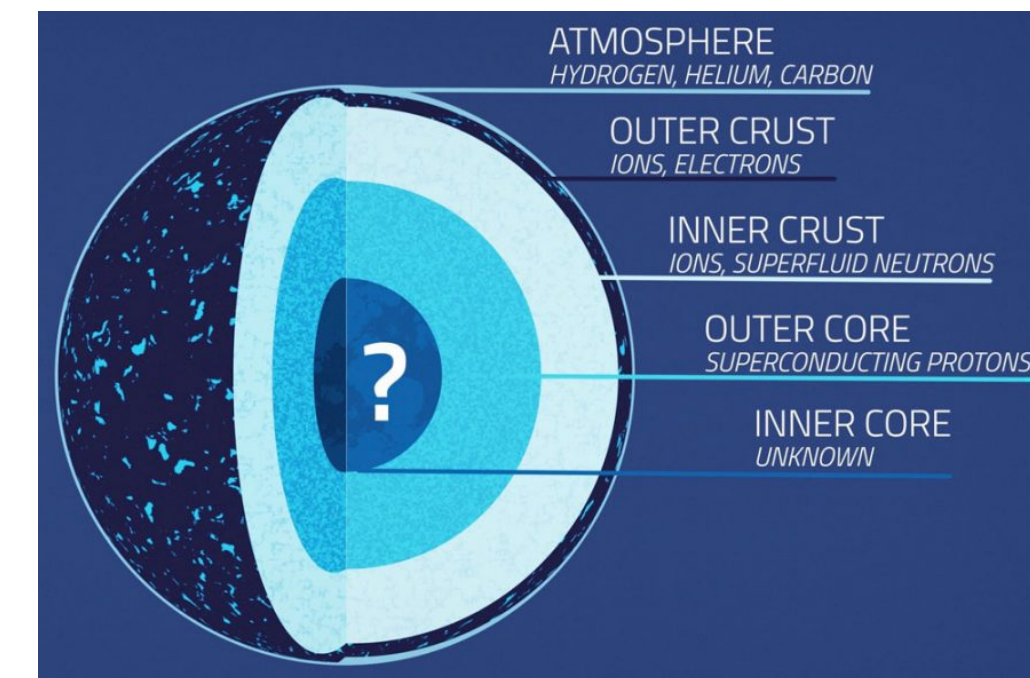


- What are hypernuclei?
 - Bound nuclear systems of non-strange and strange baryons

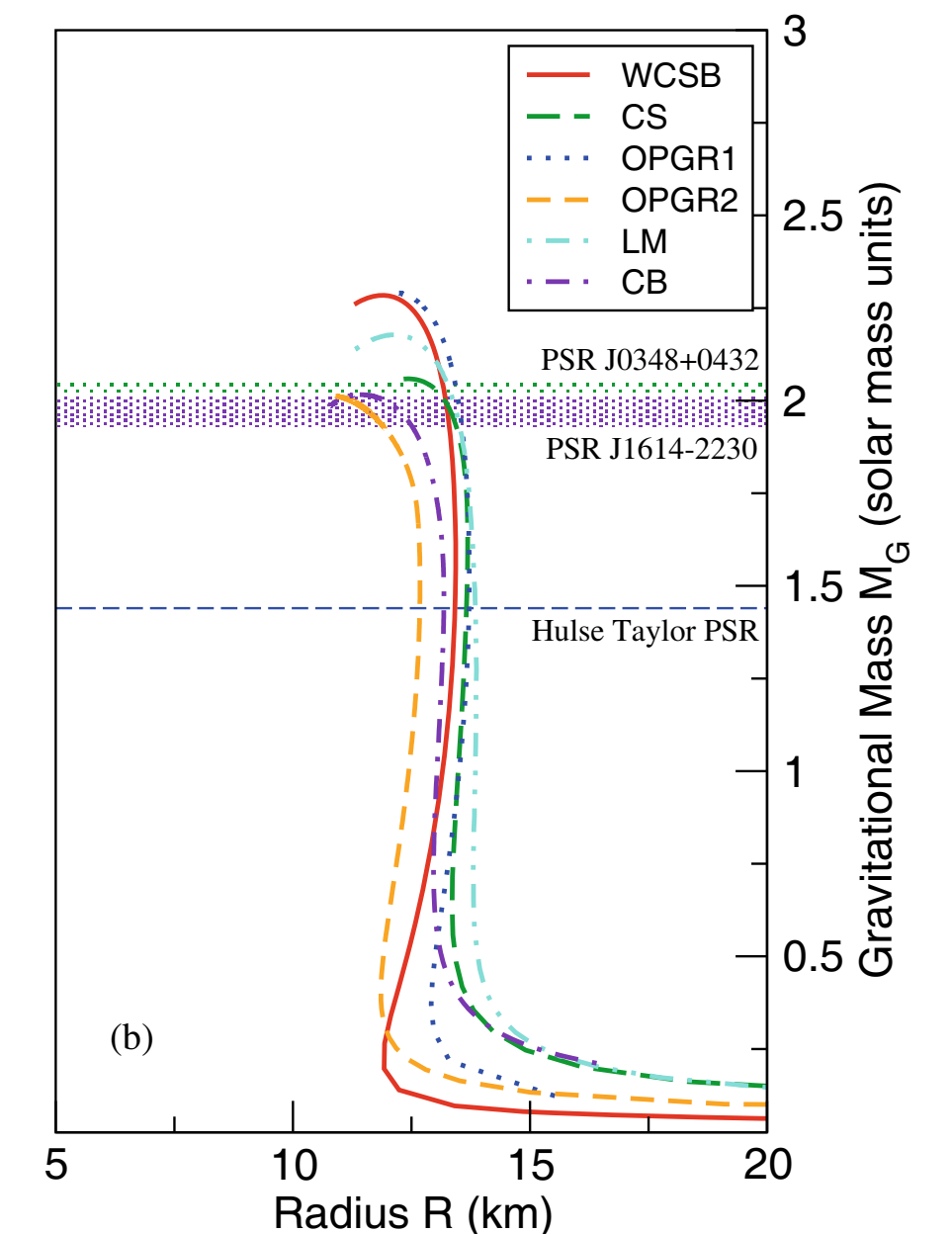


Marian Danysz (right) and Jerzy Pniewski (left) discovered hypernuclei in 1952

- Why hypernuclei?
 - Probe hyperon-nucleon (Y-N) interaction
 - Strangeness in high density nuclear matter
 - Equation-of-State (EoS) of neutron star



neutron star



D. Chatterjee, Eur. Phys. J. A (2016) 52: 29

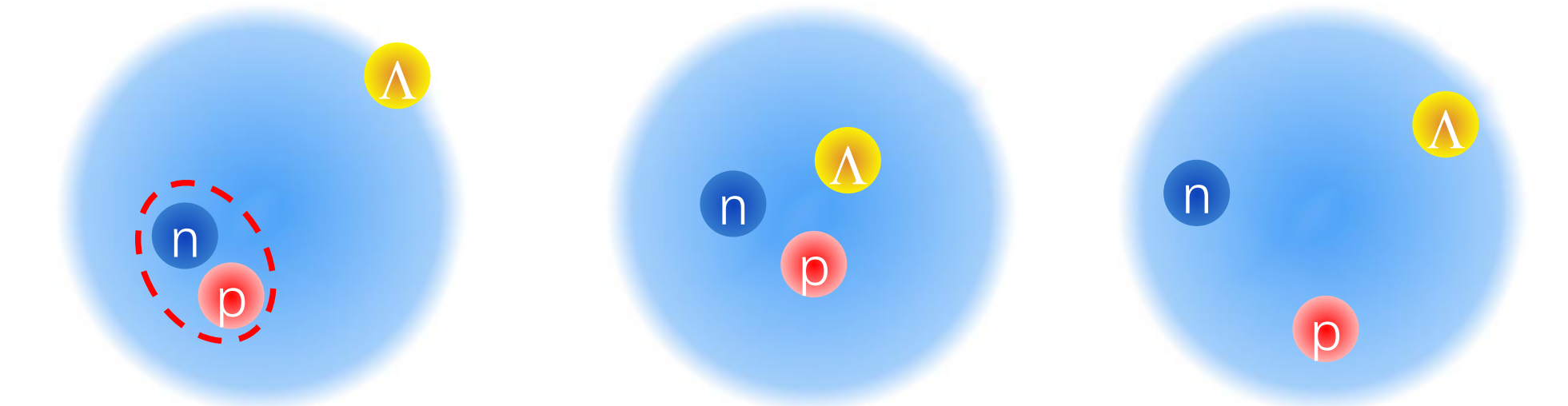
Introduction: how



- Experimentally, we can make measurements related to:

1. Internal structure

- Lifetime, binding energy, branching ratios etc.



Understanding hypernuclei structure can provide insights to the Λ -N interaction

2. Production mechanism

- Spectra, collectivity etc.

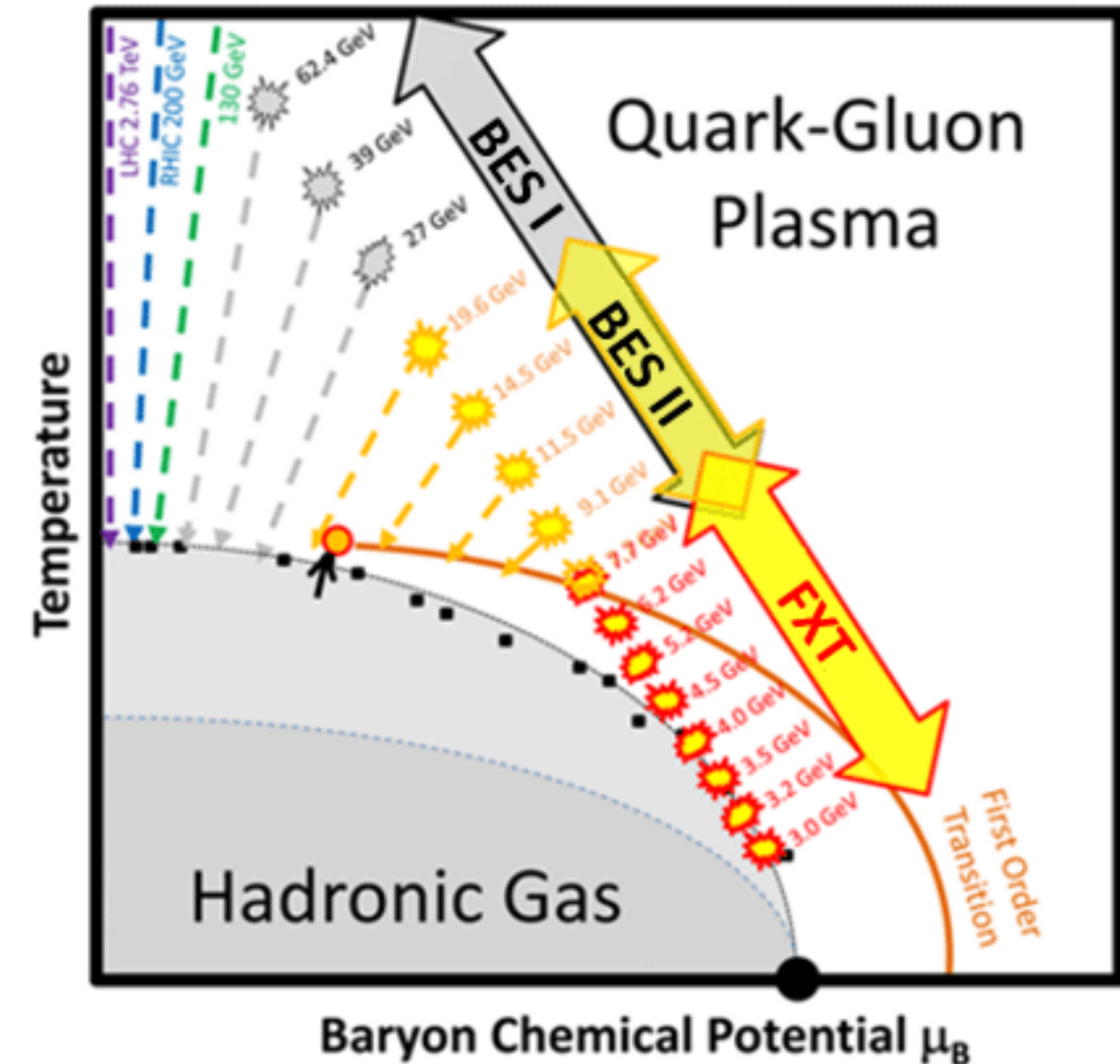
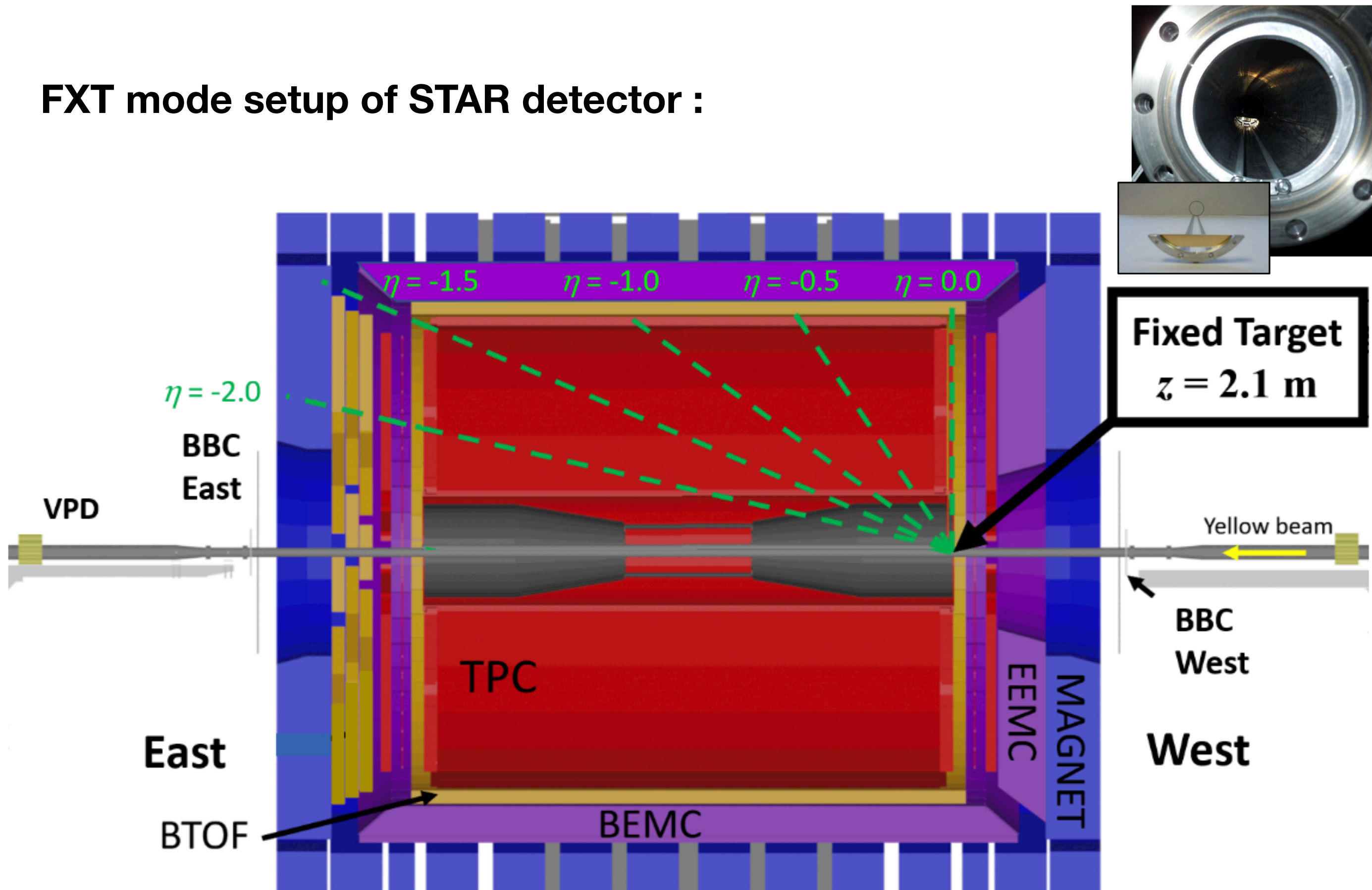
The formation of hypernuclei in violent heavy-ion collisions is not well understood

Introduction: RHIC BES program

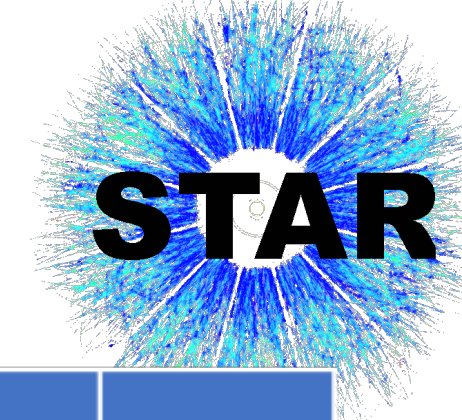


- During the BES-II program, STAR utilized the fixed-target (FXT) setup, which extends the energy reach below $\sqrt{s_{NN}} = 7.7$ GeV, down to 3.0 GeV

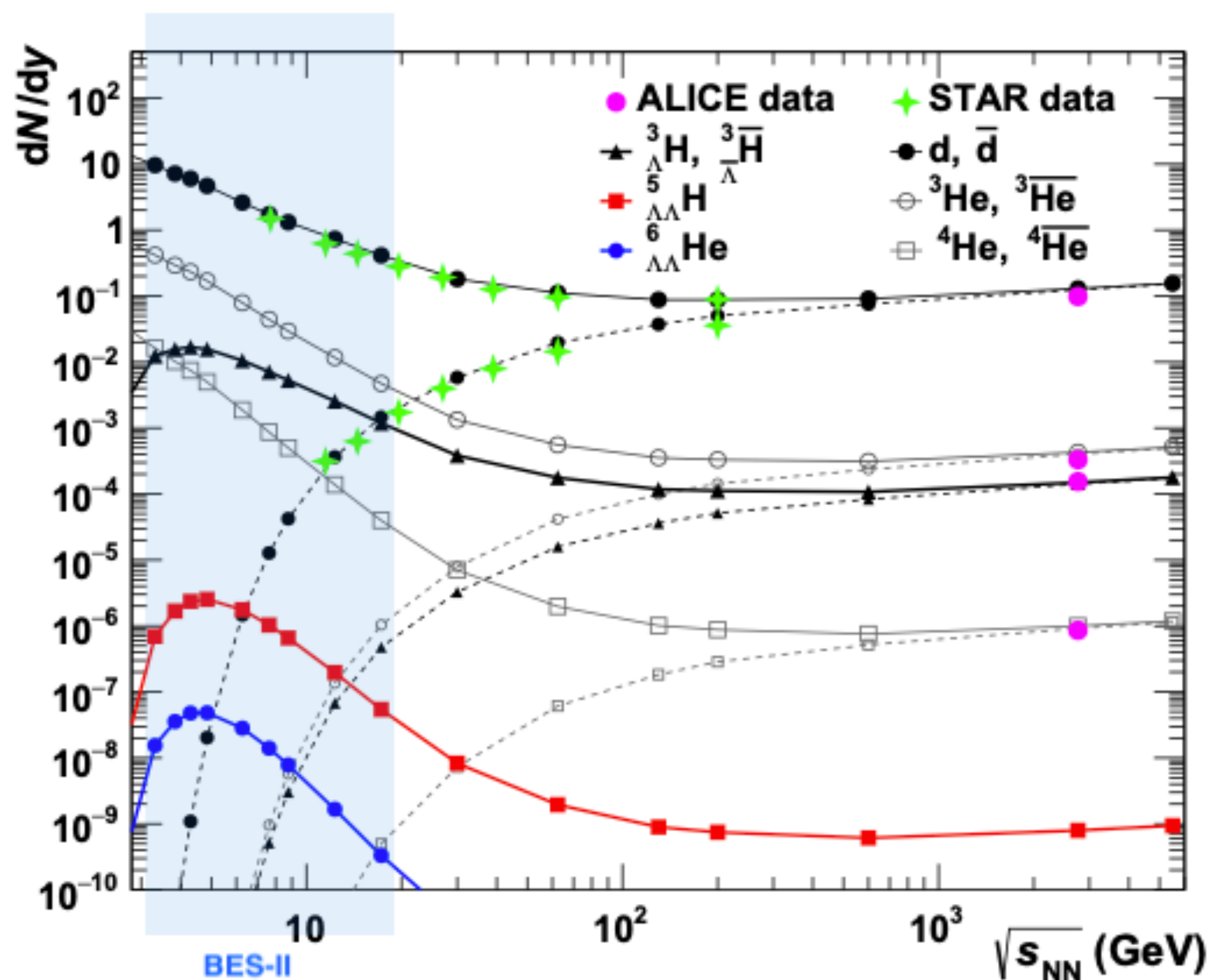
FXT mode setup of STAR detector :



Introduction: hypernuclei and STAR BES-II



- Hypernuclei measurements are scarce in heavy-ion collision experiments



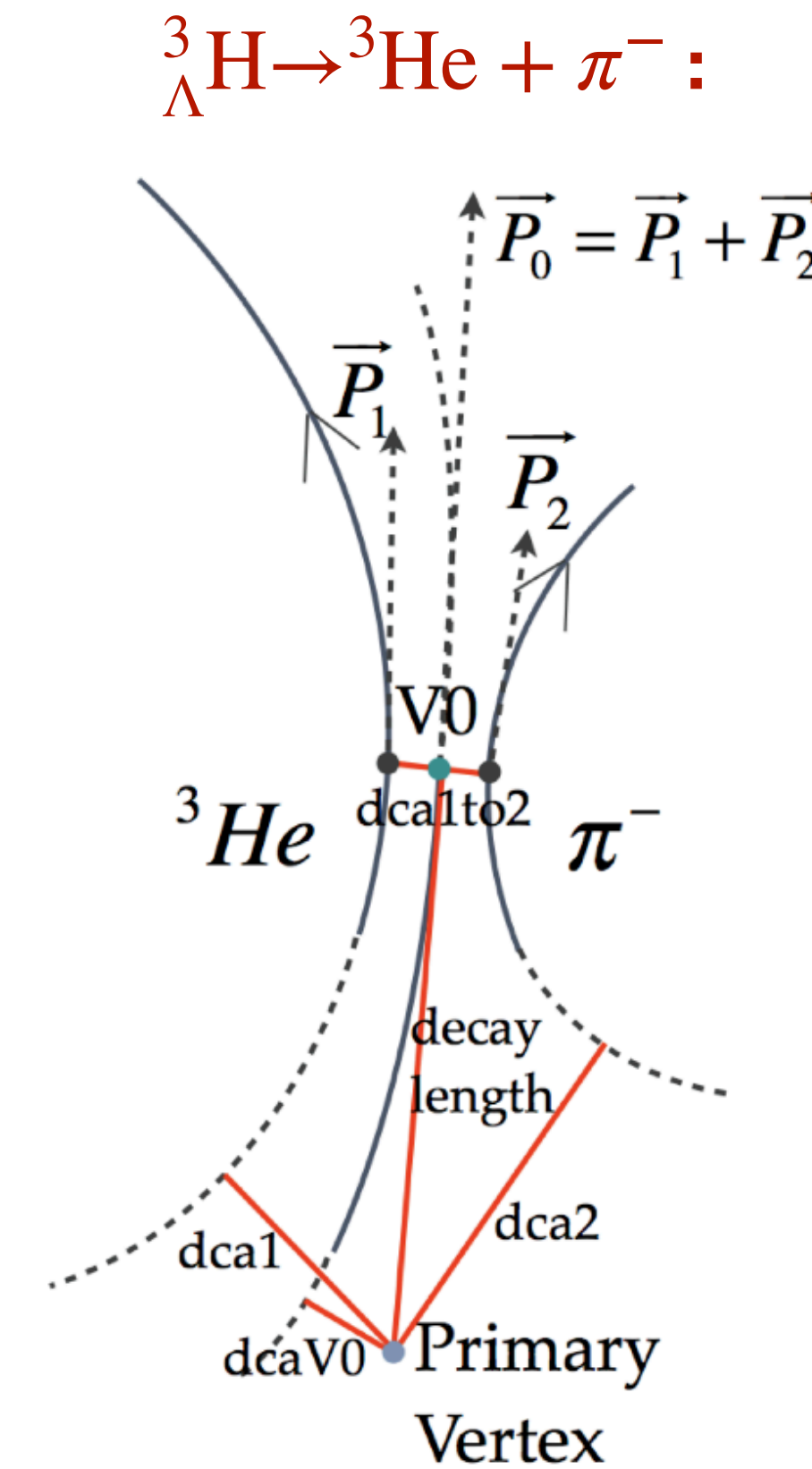
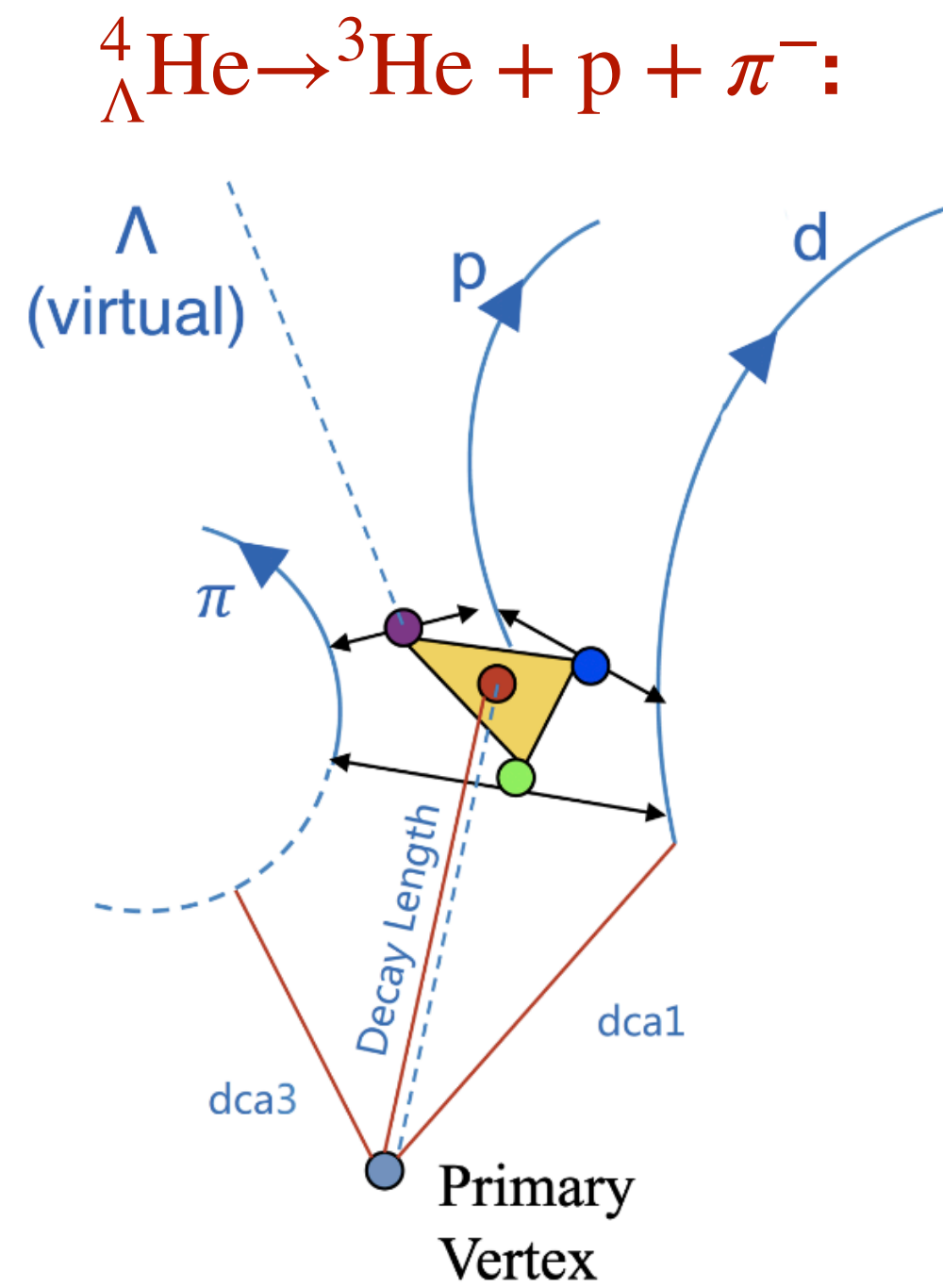
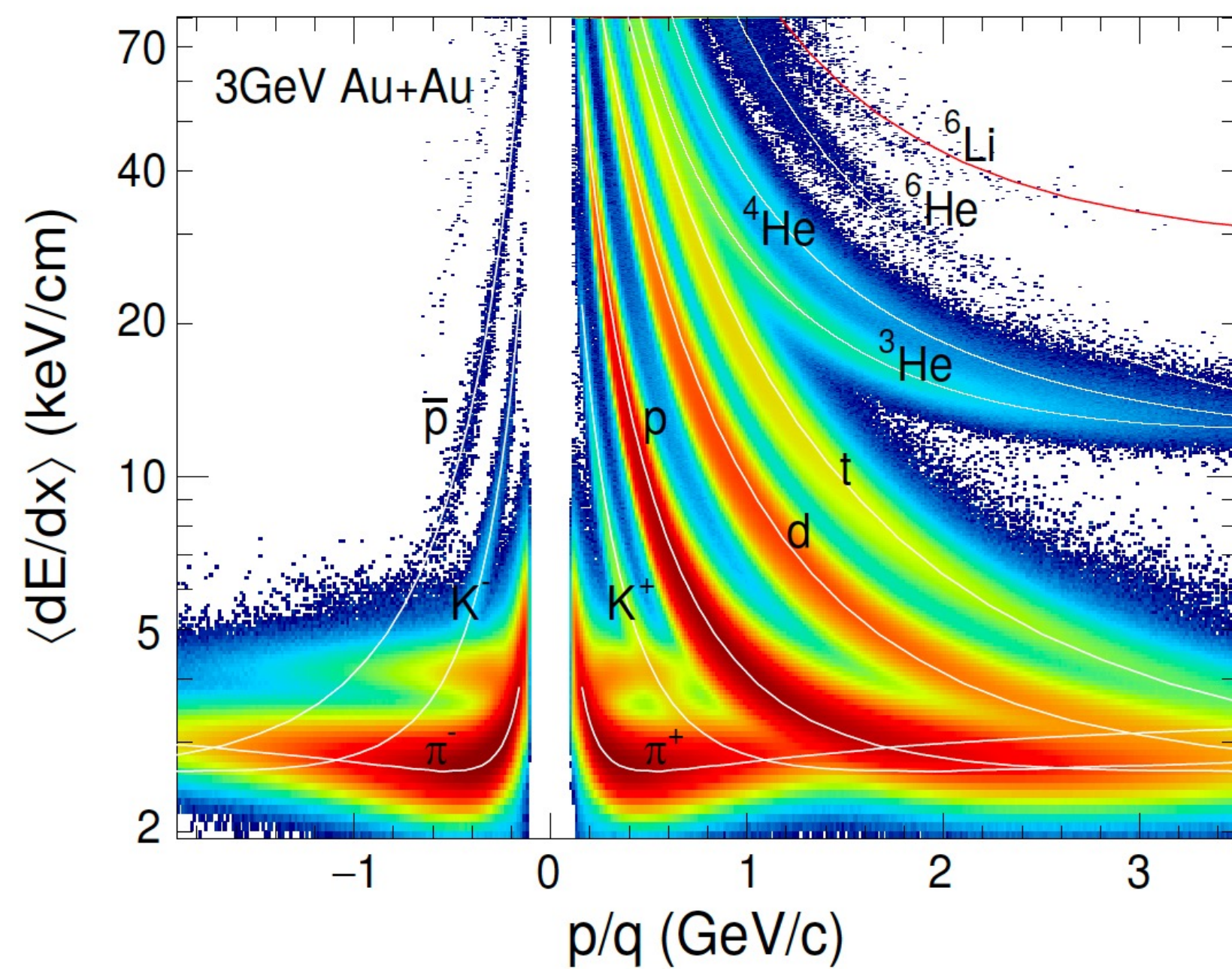
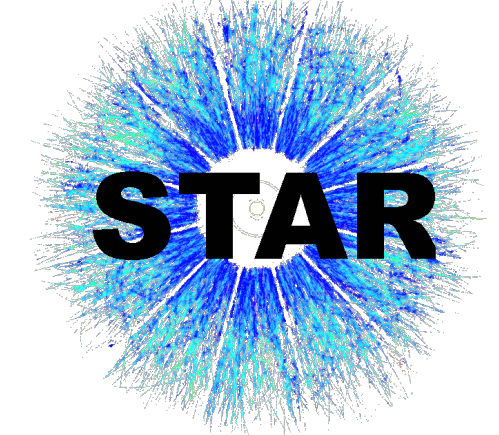
B. Dönigus, Eur. Phys. J. A (2020) 56:280
 A. Andronic et al. PLB (2011) 697:203–207

List of BES-II datasets:

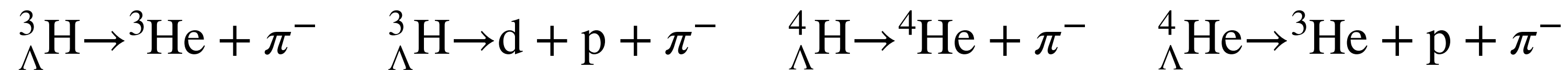
Year	$\sqrt{s_{NN}}$ [GeV]	Events
2018	27	555 M
	<u>3.0</u>	258 M
	<u>7.2</u>	155 M
2019	19.6	478 M
	14.6	324 M
	<u>3.9</u>	53 M
	<u>3.2</u>	201 M
	<u>7.7</u>	51 M
2020	11.5	235 M
	<u>7.7</u>	113 M
	<u>4.5</u>	108 M
	<u>6.2</u>	118 M
	<u>5.2</u>	103 M
	<u>3.9</u>	117 M
	<u>3.5</u>	116 M
	9.2	162 M
2021	<u>7.2</u>	317 M
	7.7	101 M
	<u>3.0</u>	2103 M
	<u>9.2</u>	54 M
	<u>11.5</u>	52 M
	<u>13.7</u>	51 M
	17.3	256 M
	<u>7.2</u>	89 M

- At low beam energies, hypernuclei production is expected to be enhanced due to high baryon density
 - Datasets with large statistics taken during BES-II
- BES-II is a great opportunity to study hypernuclei production

Particle identification and hypernuclei reconstruction

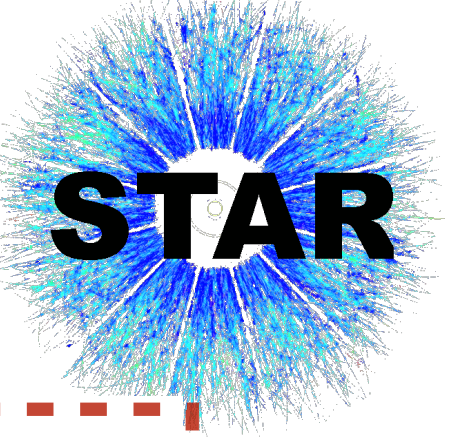


- Particle identification from energy loss measurement using TPC
- KF particle package^[1] is used for signal reconstruction
- Hypernuclei reconstructed via their weak decay channels:



[1]Zyzak M, Kisel I, Senger P. Online selection of short-lived particles on many-core computer architectures in the CBM experiment at FAIR[R]. Collaboration FAIR: CBM, 2016.

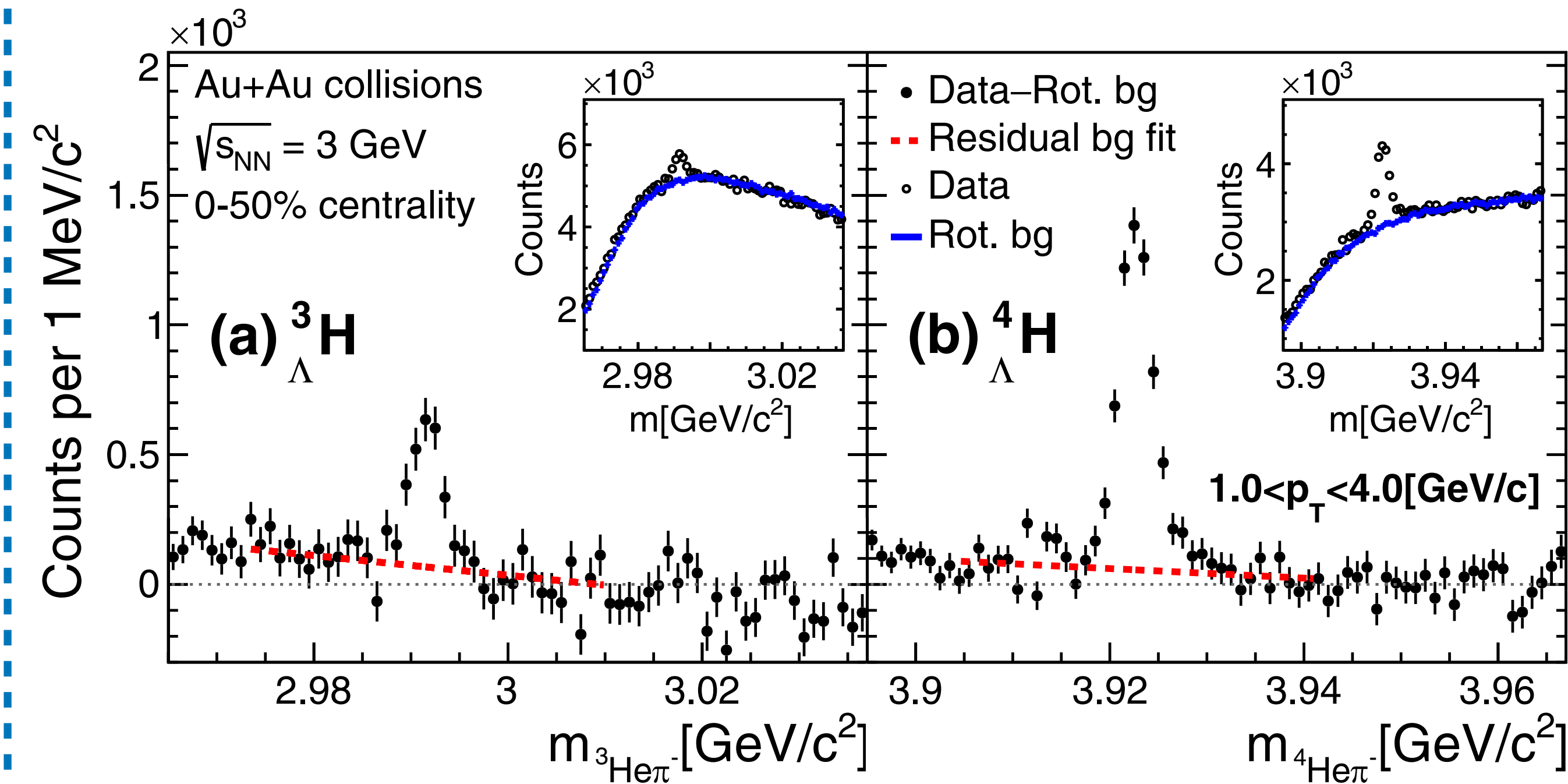
Hypernuclei signal reconstruction



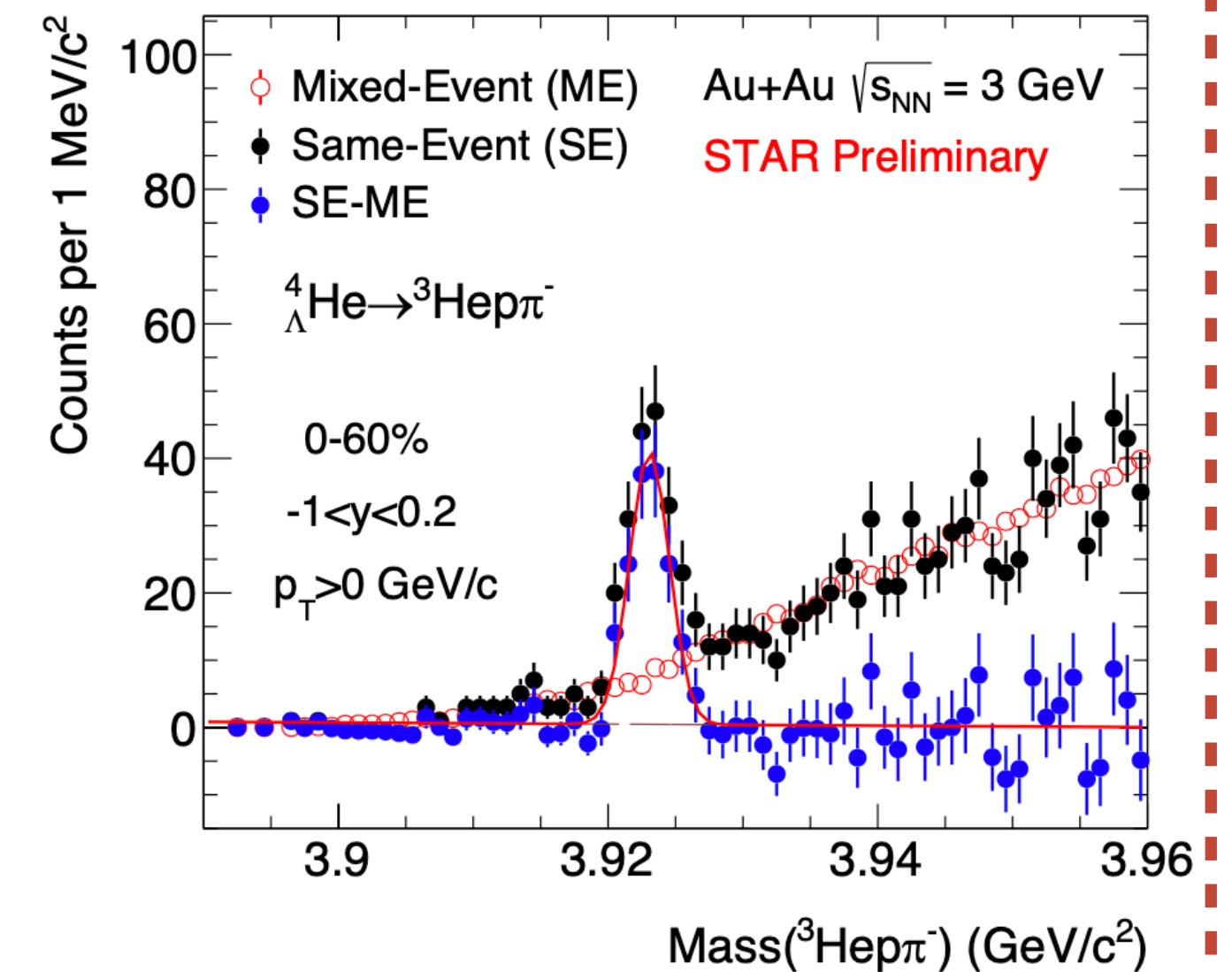
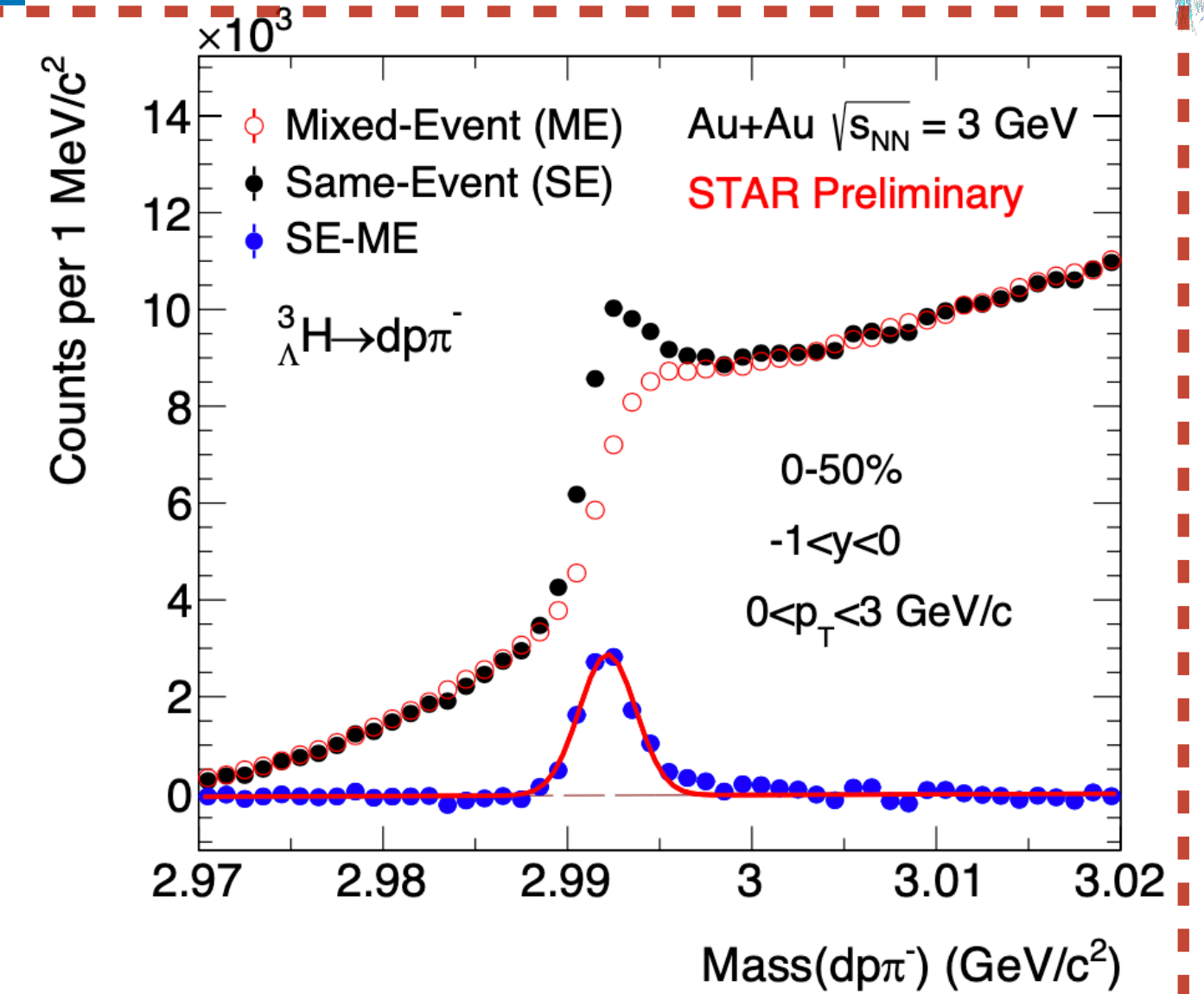
2-body decay channels:

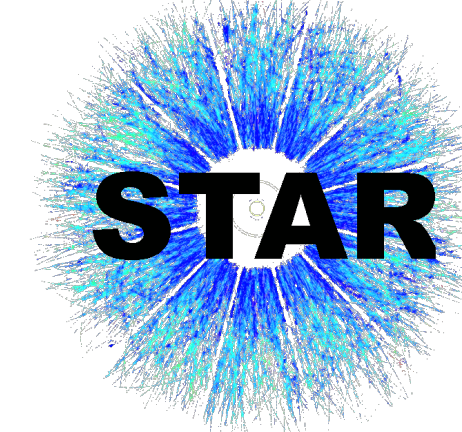
STAR, PRL 128, 202301(2022)

3-body decay channels:



- Combinatorial background estimated via:
 - Rotating pion tracks for 2-body decay channels
 - Event mixing for 3-body decay channels

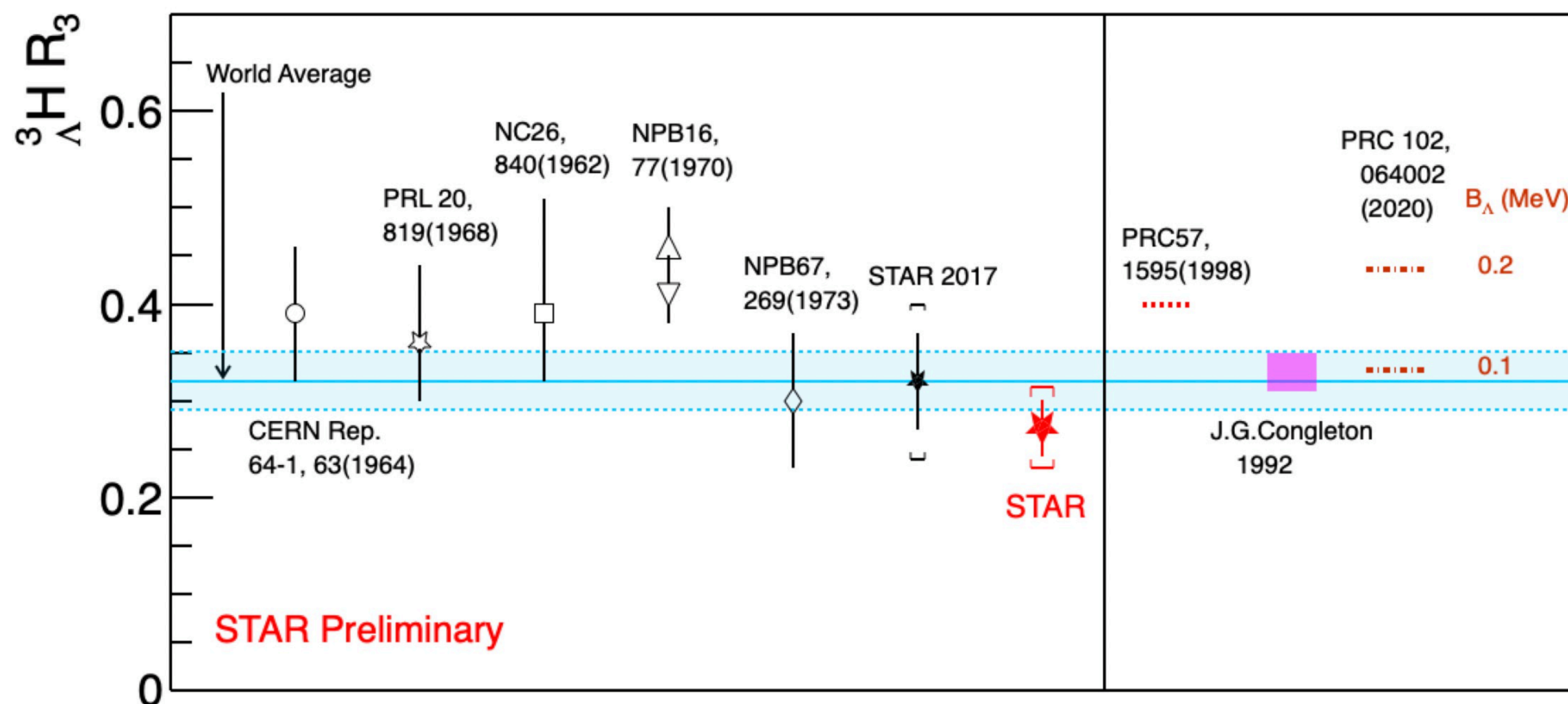




${}^3_{\Lambda}\text{H}$ branching ratio R_3

Relative branching ratio: $R_3 = \frac{\text{B.R.}({}^3_{\Lambda}\text{H} \rightarrow {}^3\text{He}\pi^-)}{\text{B.R.}({}^3_{\Lambda}\text{H} \rightarrow {}^3\text{He}\pi^-) + \text{B.R.}({}^3_{\Lambda}\text{H} \rightarrow \text{dp}\pi^-)}$

F. Hildenbrand et al. PRC 102, 064002 (2020)

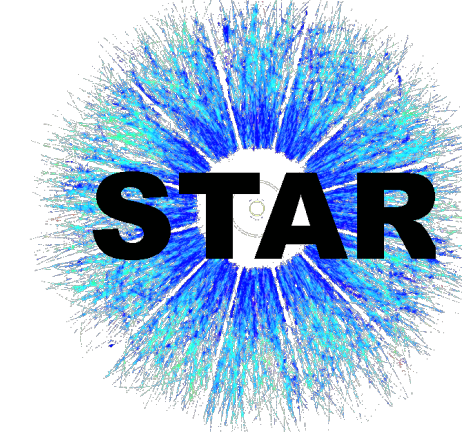


- Recent calculation shows that R_3 may be sensitive to the binding energy (B_{Λ}) of ${}^3_{\Lambda}\text{H}$
 - $B_{\Lambda} \rightarrow$ provide constraints to Y-N interaction

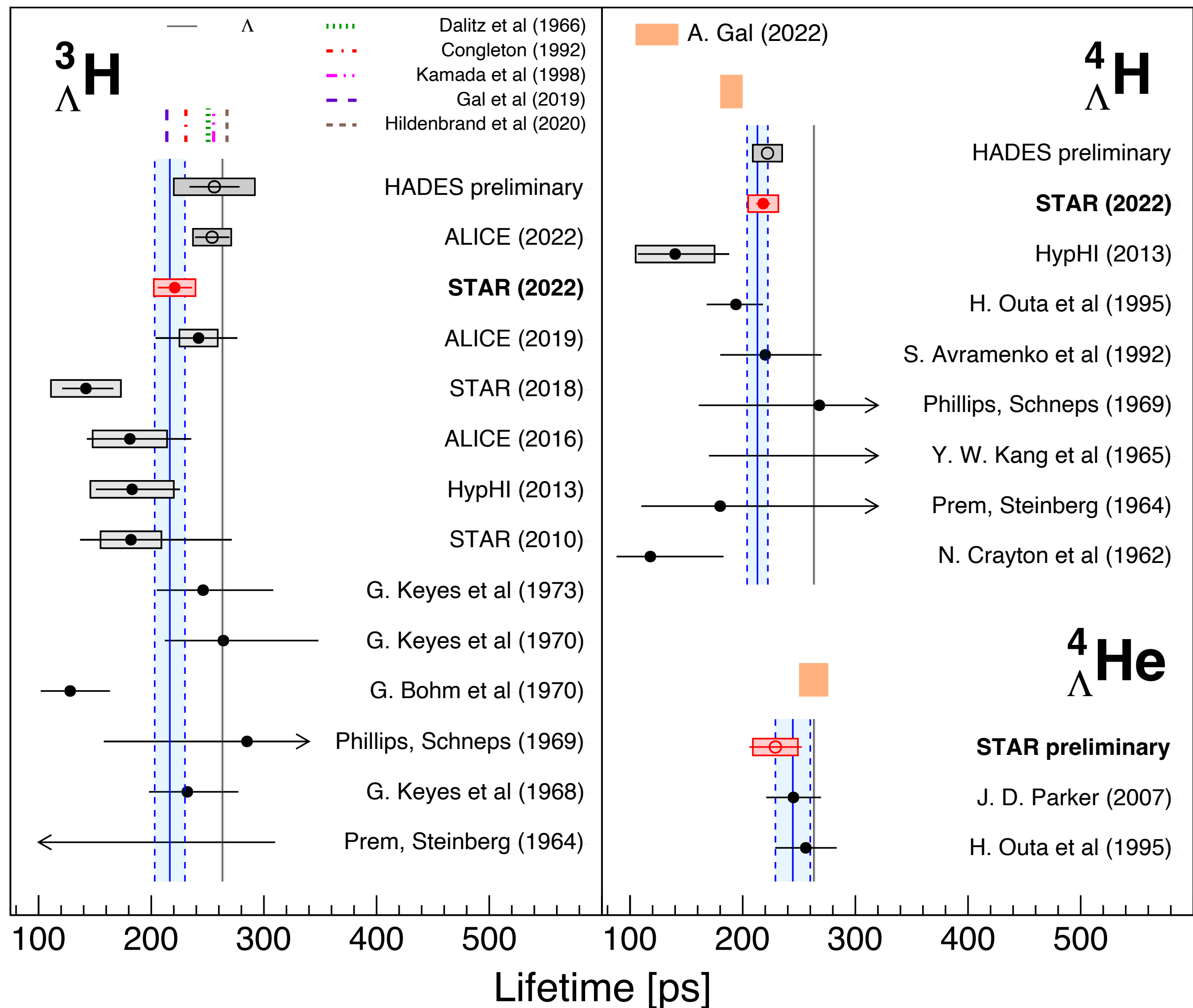
- Using $\sqrt{s_{NN}} = 3.0$ GeV data:
 - $R_3 = 0.272 \pm 0.030(\text{stat.}) \pm 0.042(\text{syst.})$
 - Updated world average R_3 (0.32 ± 0.03) is consistent with theoretical models assuming $B_{\Lambda} \sim 0.1$ MeV

- Improved precision on R_3
 - Stronger constraints on absolute B.R.s and hypertriton internal structure models

${}^3_{\Lambda}\text{H}$, ${}^4_{\Lambda}\text{H}$ and ${}^4_{\Lambda}\text{He}$ lifetimes



STAR, PRL 128, 202301(2022)



Using $\sqrt{s_{NN}} = 3.0 \text{ GeV}$ and 7.2 GeV datasets:

${}^3_{\Lambda}\text{H}: \tau = 221 \pm 15(\text{stat.}) \pm 19(\text{syst.})[\text{ps}]$

${}^4_{\Lambda}\text{H}: \tau = 218 \pm 6(\text{stat.}) \pm 13(\text{syst.})[\text{ps}]$

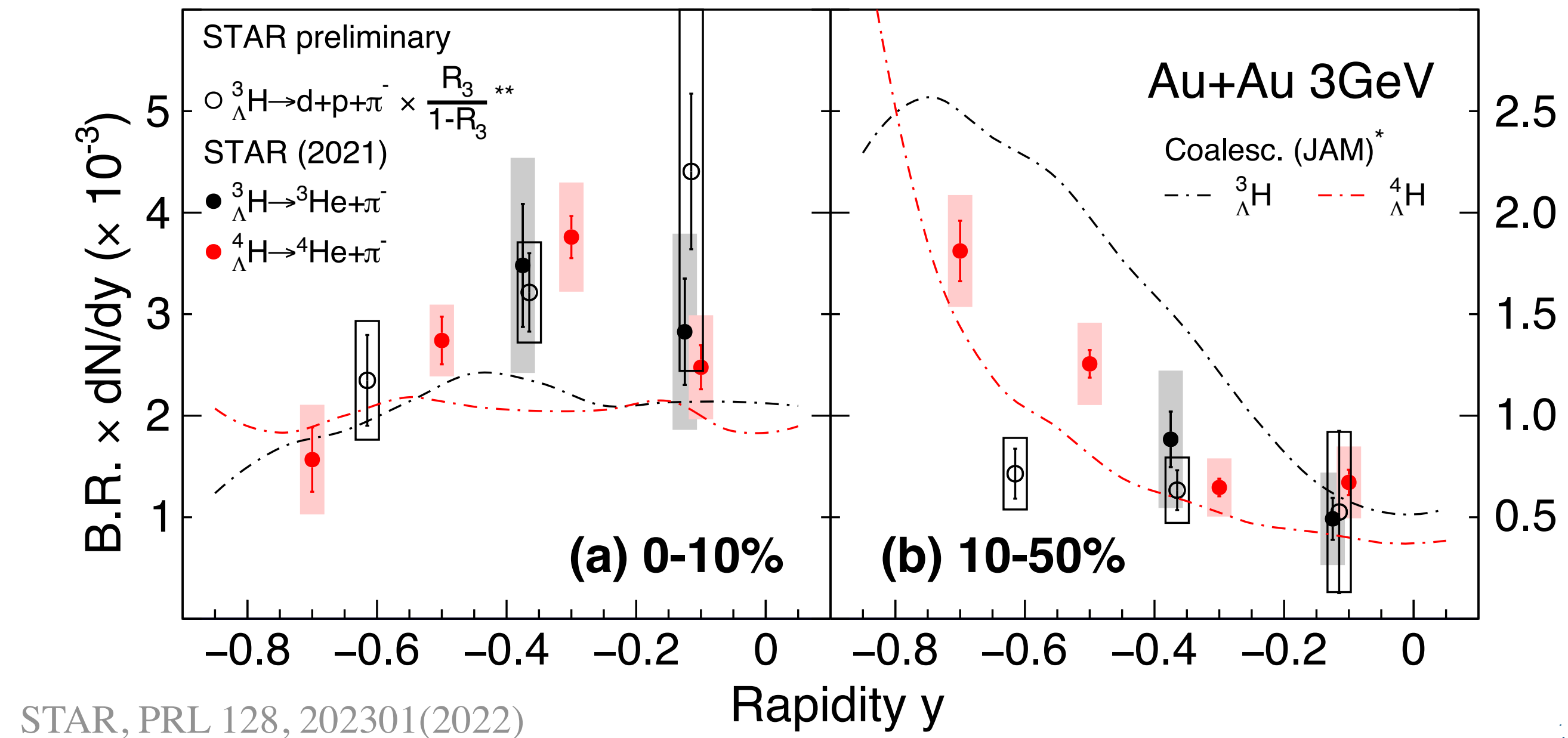
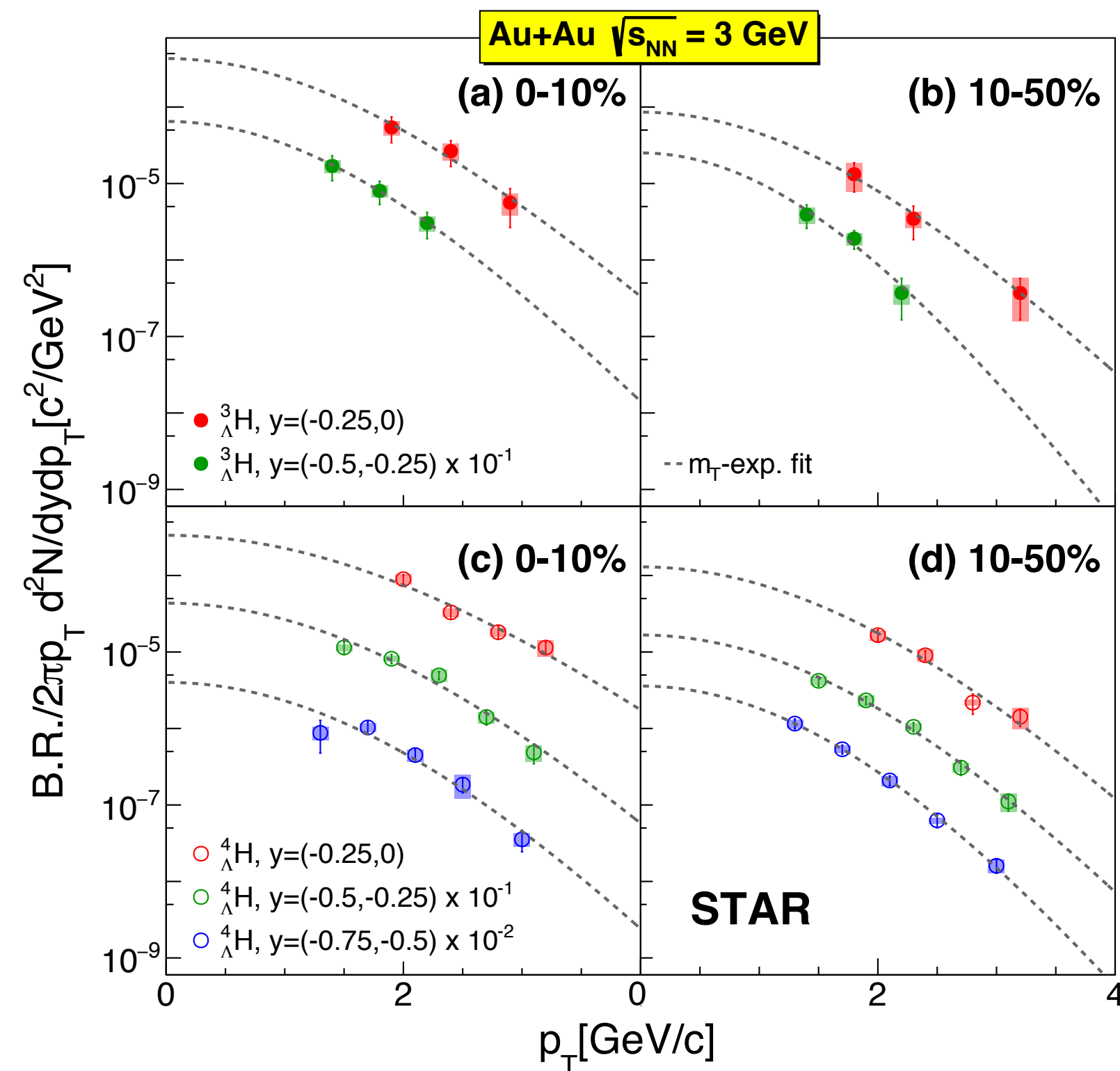
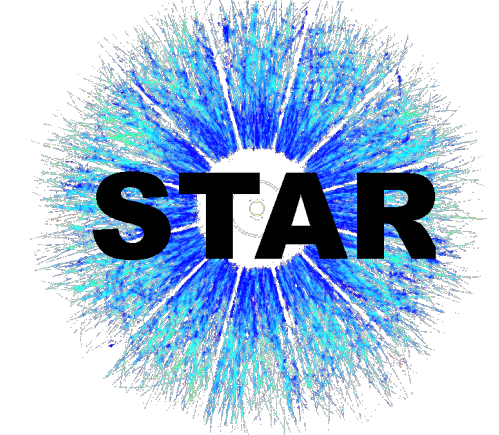
${}^4_{\Lambda}\text{He}: \tau = 229 \pm 23(\text{stat.}) \pm 20(\text{syst.})[\text{ps}]$

- Lifetimes of light hypernuclei ${}^3_{\Lambda}\text{H}$, ${}^4_{\Lambda}\text{H}$ and ${}^4_{\Lambda}\text{He}$ are shorter than that of free Λ (with 1.8σ , 3.0σ , 1.1σ respectively)
- Consistent with former measurements (within 2.5σ for ${}^3_{\Lambda}\text{H}$, ${}^4_{\Lambda}\text{H}$)
- $\tau_{{}^3_{\Lambda}\text{H}}$: consistent with calculation including pion FSI^[1] and calculation with Λd 2-body picture^[2] within 1σ
- $\tau_{{}^4_{\Lambda}\text{H}}$ and $\tau_{{}^4_{\Lambda}\text{He}}$: consistent with expectations from isospin rule

${}^3_{\Lambda}\text{H}$, ${}^4_{\Lambda}\text{H}$ results with improved precision
 → Provide tighter constraints on models.

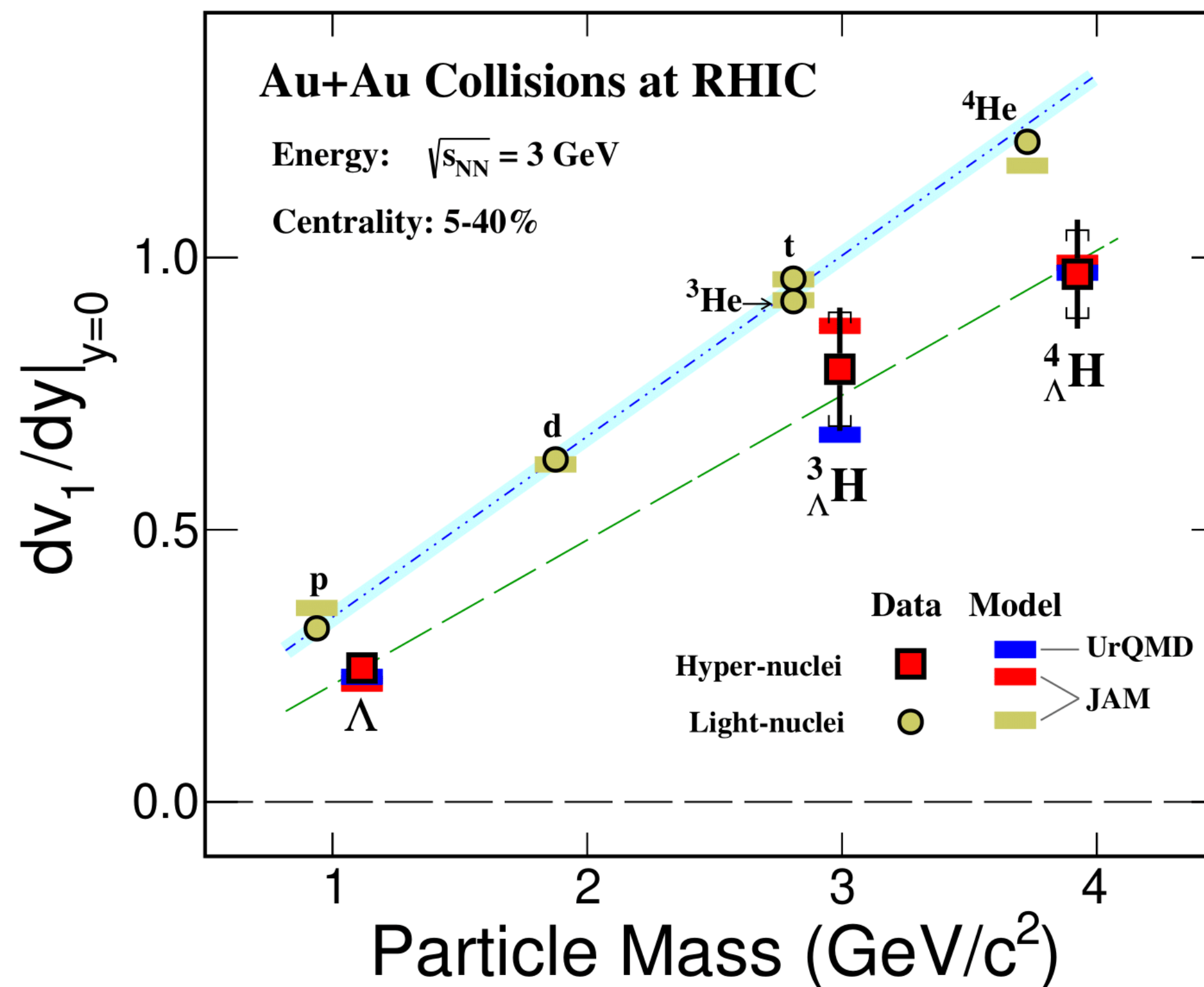
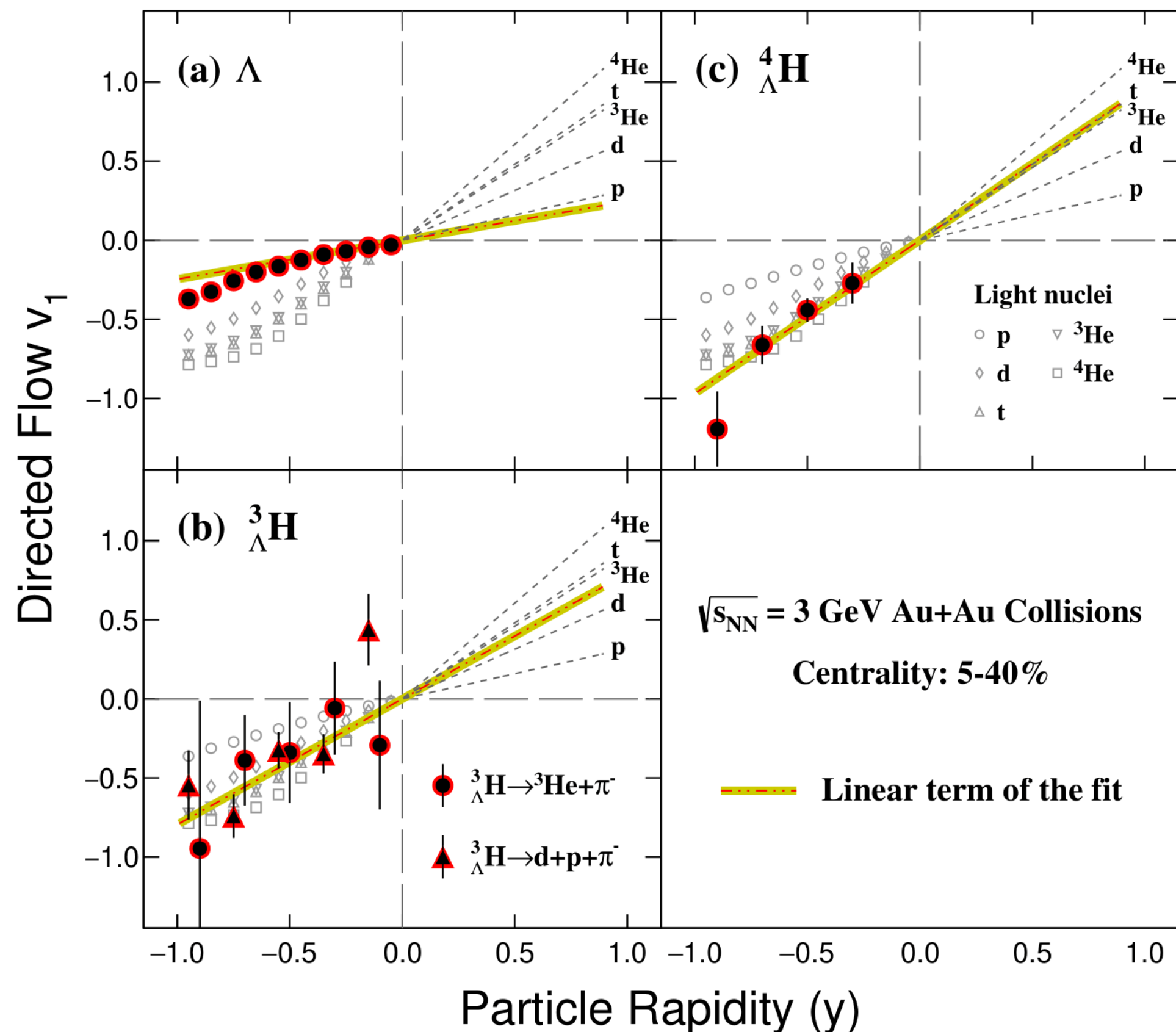
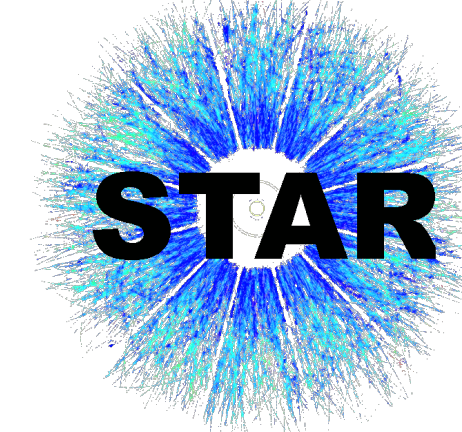
[1]A. Gal and H. Garcilazo, PLB 791, 48 (2019)
 [2]J.G. Congleton, J. Phys. G 18, 339 (1992)

Hypernuclei production at 3 GeV



- Different trends in the ${}^4_{\Lambda}H$ rapidity distribution in central (0-10%) and mid-central (10-50%) collisions at $\sqrt{s_{NN}} = 3.0$ GeV
- Transport model (JAM) with coalescence approximately reproduces trends of ${}^4_{\Lambda}H$ rapidity distributions seen in data

${}^3_{\Lambda}\text{H}$ and ${}^4_{\Lambda}\text{H}$ directed flow at 3 GeV

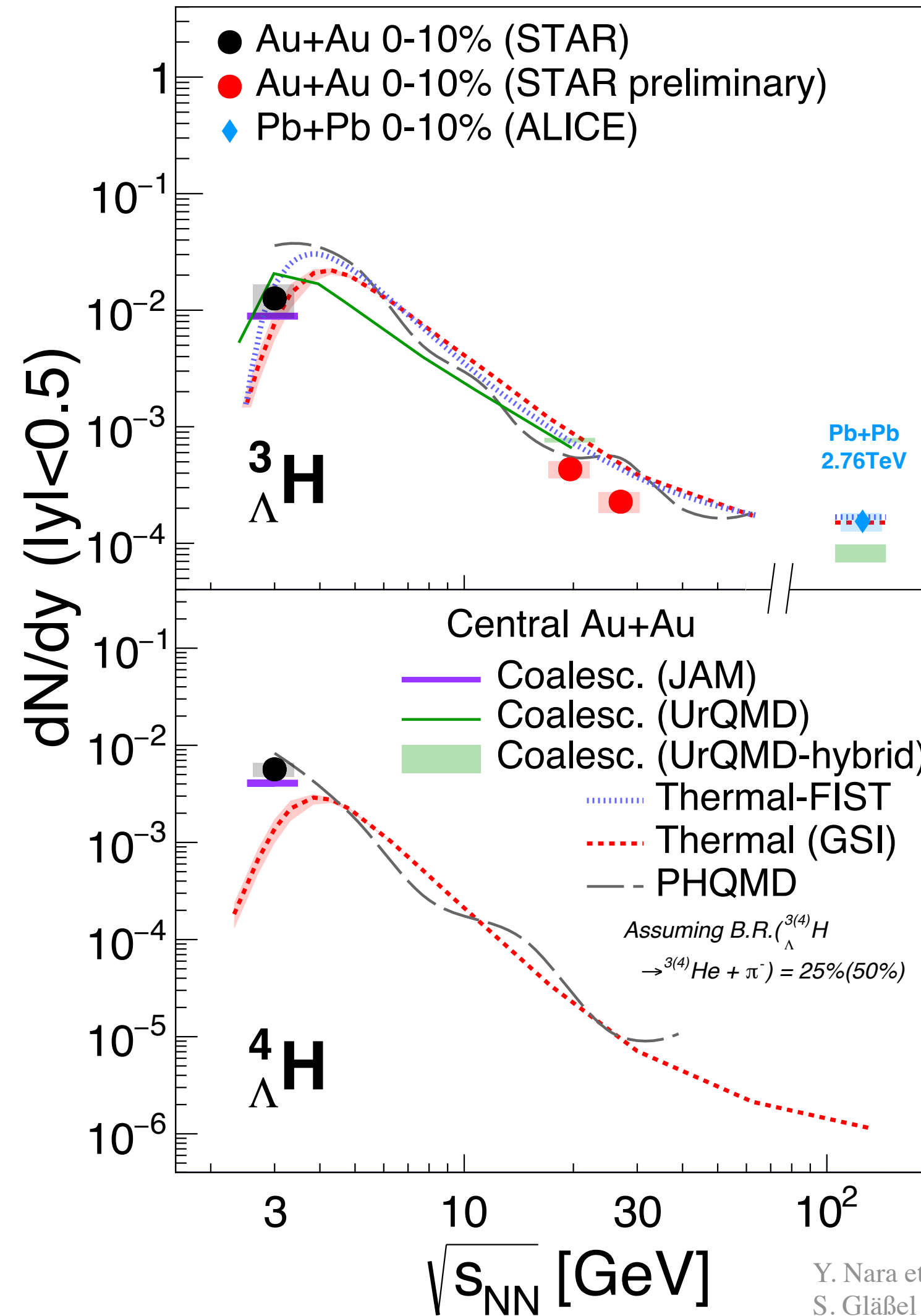
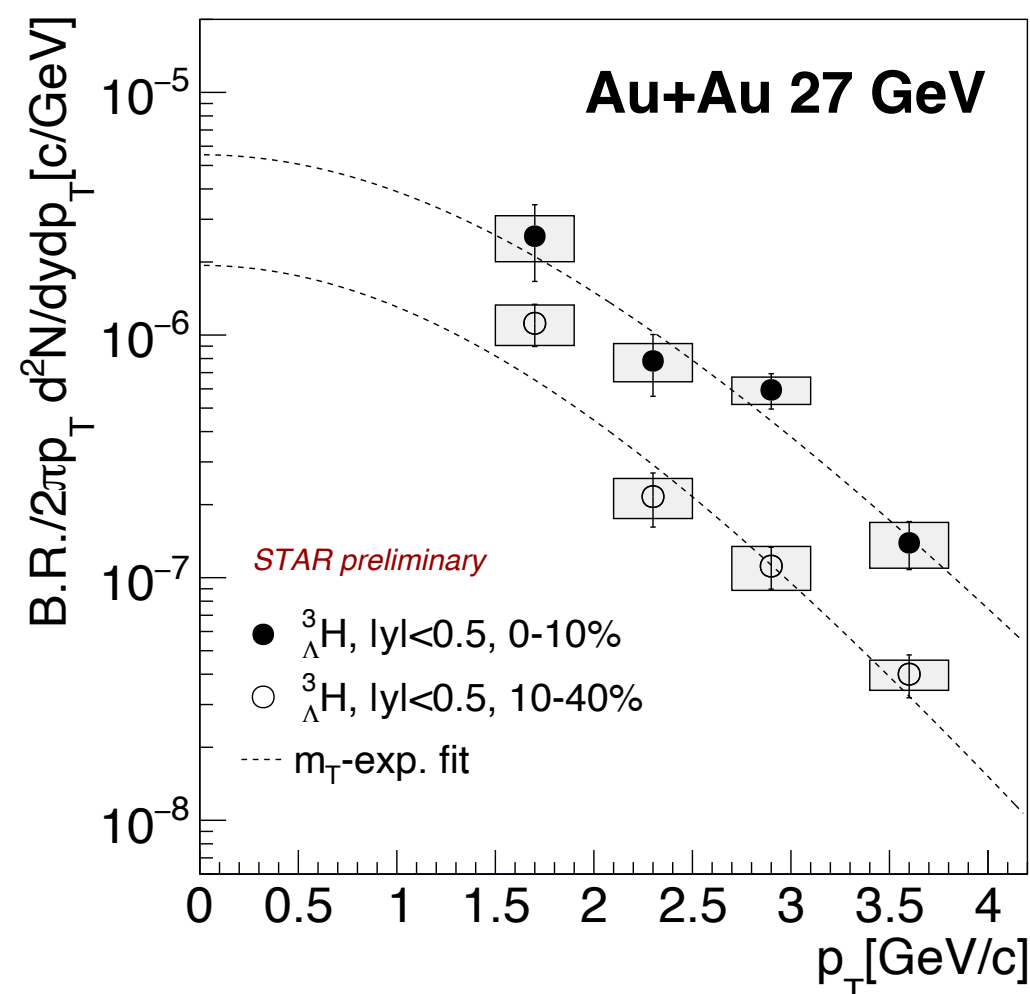
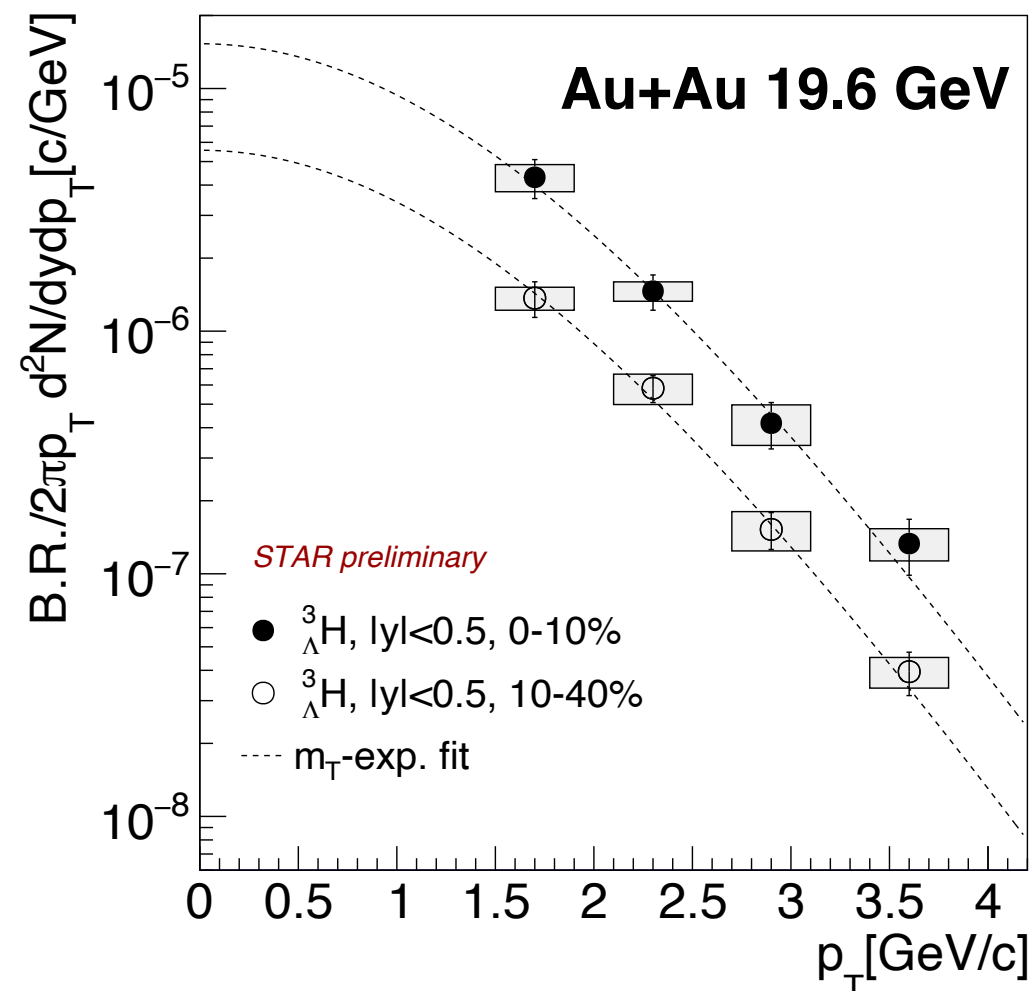
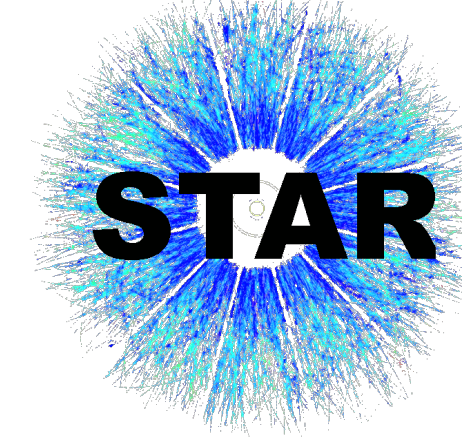


To be submitted to arXiv soon

- First measurements of ${}^3_{\Lambda}\text{H}$ and ${}^4_{\Lambda}\text{H}$ directed flow (v_1) in 5-40% central Au+Au collisions at 3 GeV
- v_1 slopes of ${}^3_{\Lambda}\text{H}$ and ${}^4_{\Lambda}\text{H}$ follow mass number scaling.

→ Imply **coalescence** process to be the dominant formation mechanism for hypernuclei in heavy-ion collisions

Energy dependence of hypernuclei production in heavy-ion collisions



STAR, PRL 128 (2022) 202301
ALICE, PLB 754 (2016) 360

Y. Nara et al, PRC 61 (1999) 024901 (JAM)
S. Gläsel et al, arXiv: 2106.14839 (PHQMD)
A. Andronic et al, PLB 697 (2011) 203 (Thermal (GSI))
T. Reichert, J. Steinheimer et al, arXiv:2210.11876(2022) (UrQMD, Thermal-FIST)

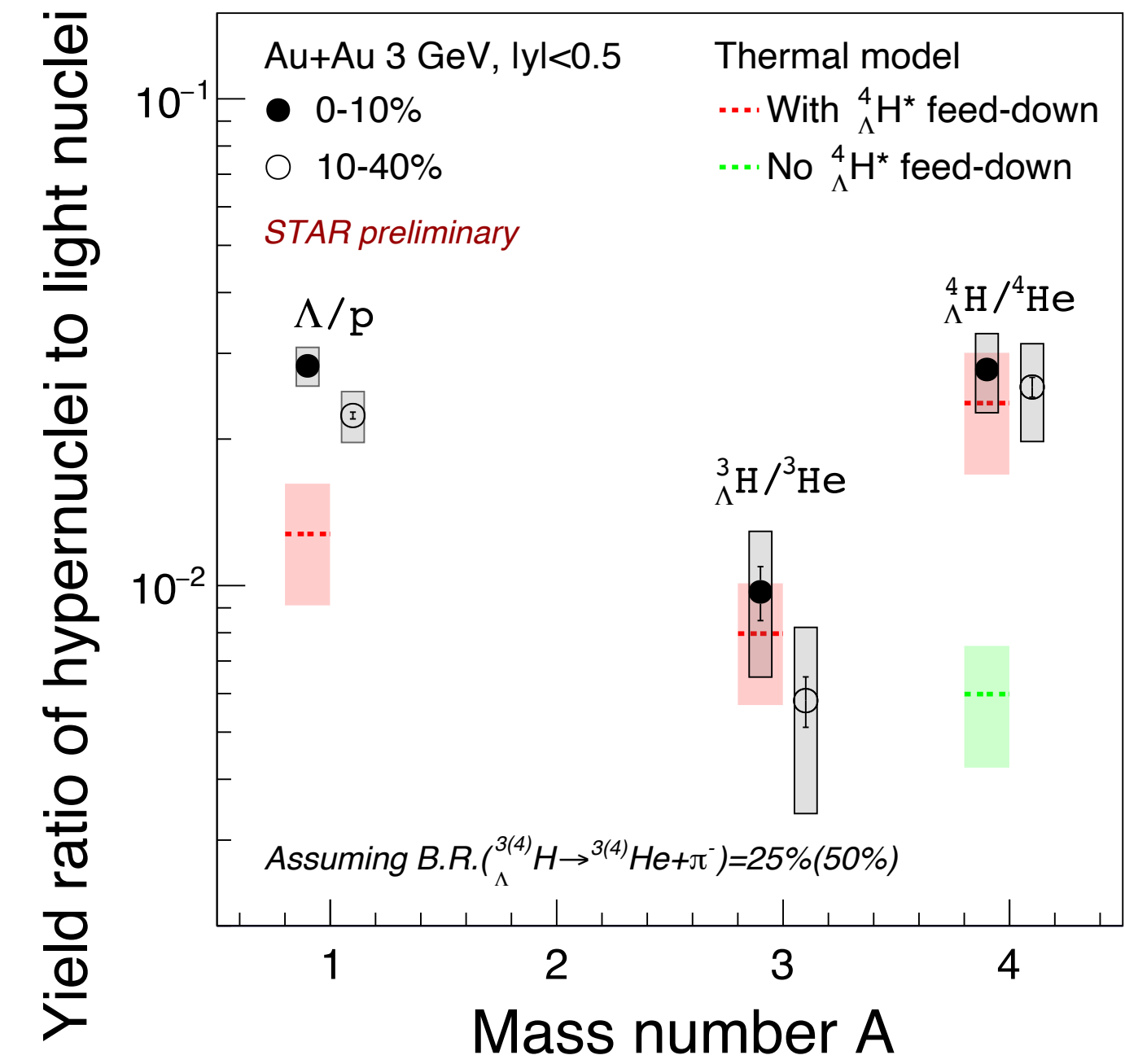
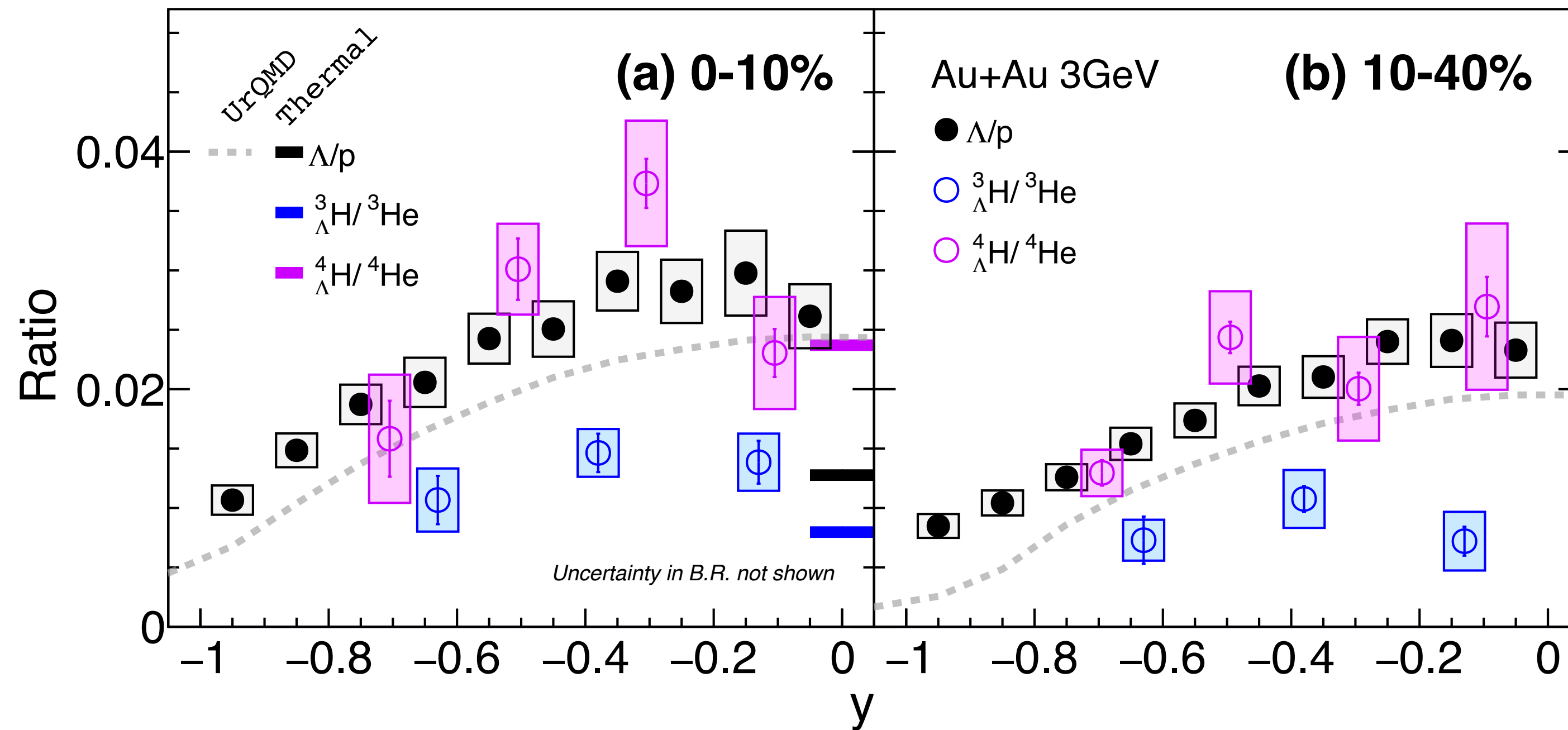
- ${}^3_{\Lambda}\text{H}$ yield at mid-rapidity increases from 2.76 TeV to 3 GeV
 - Driven by increase in baryon density at low energies
- Thermal(GSI), Coalescence(UrQMD), Thermal-FIST and PHQMD reproduce the trend

For Au+Au @ 3 GeV

- Coalescence(JAM) with tuned coalescence parameters can describe data
- PHQMD describes ${}^4_{\Lambda}\text{H}$, but slightly overestimates ${}^3_{\Lambda}\text{H}$

Provide first constraints for hypernuclei production models in the high-baryon-density region

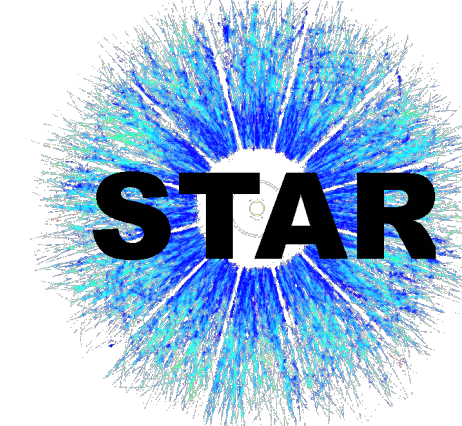
Hyper-to-light nuclei ratios



- **Suppression of ${}^3_{\Lambda}\text{H}/{}^3\text{He}$ yield ratios compared to that of Λ/p**
 - Observed at both 0-10% and 10-40% centrality in Au+Au collisions at 3 GeV.
- **The ${}^4_{\Lambda}\text{H}/{}^4\text{He}$ yield ratios are comparable to that of Λ/p**
- **Thermal model calculations including excited ${}^4_{\Lambda}\text{H}^*$ feed-down show a similar trend**
 - Feed-down from excited state enhances ${}^4_{\Lambda}\text{H}$ production
- **Support creation of excited A=4 hypernuclei in heavy-ion collisions**

A. Andronic et al, PLB 697 (2011) 203 (Thermal model)

$S_{3,4}$ at 3 GeV



- **Strangeness population factor S_A**

- Relative suppression of hypernuclei production compared to light nuclei production

$$S_A = \frac{\Lambda^A \text{H}}{\Lambda^A \text{He} \times \frac{\Lambda}{p}} = \frac{B_A(\Lambda^A \text{H})(p_T)}{B_A(\Lambda^A \text{He})(p_T)}$$

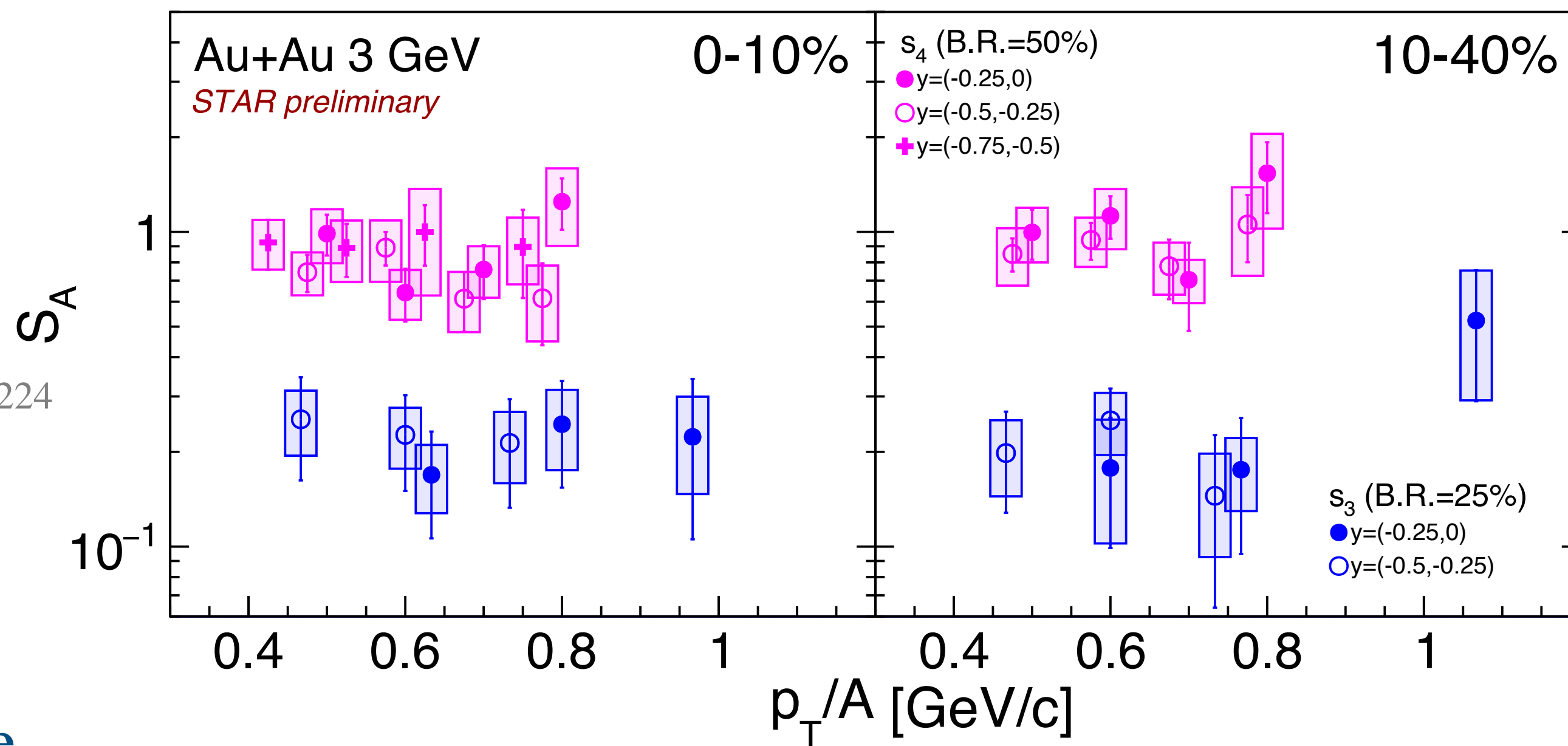
S.Zhang, PLB 684(2010)224

- B_A : Coalescence parameters

- Expect ~ 1 if no suppression

$S_3 < 1 \rightarrow$ relative suppression of ${}^3_\Lambda \text{H}$ to ${}^3\text{He}$

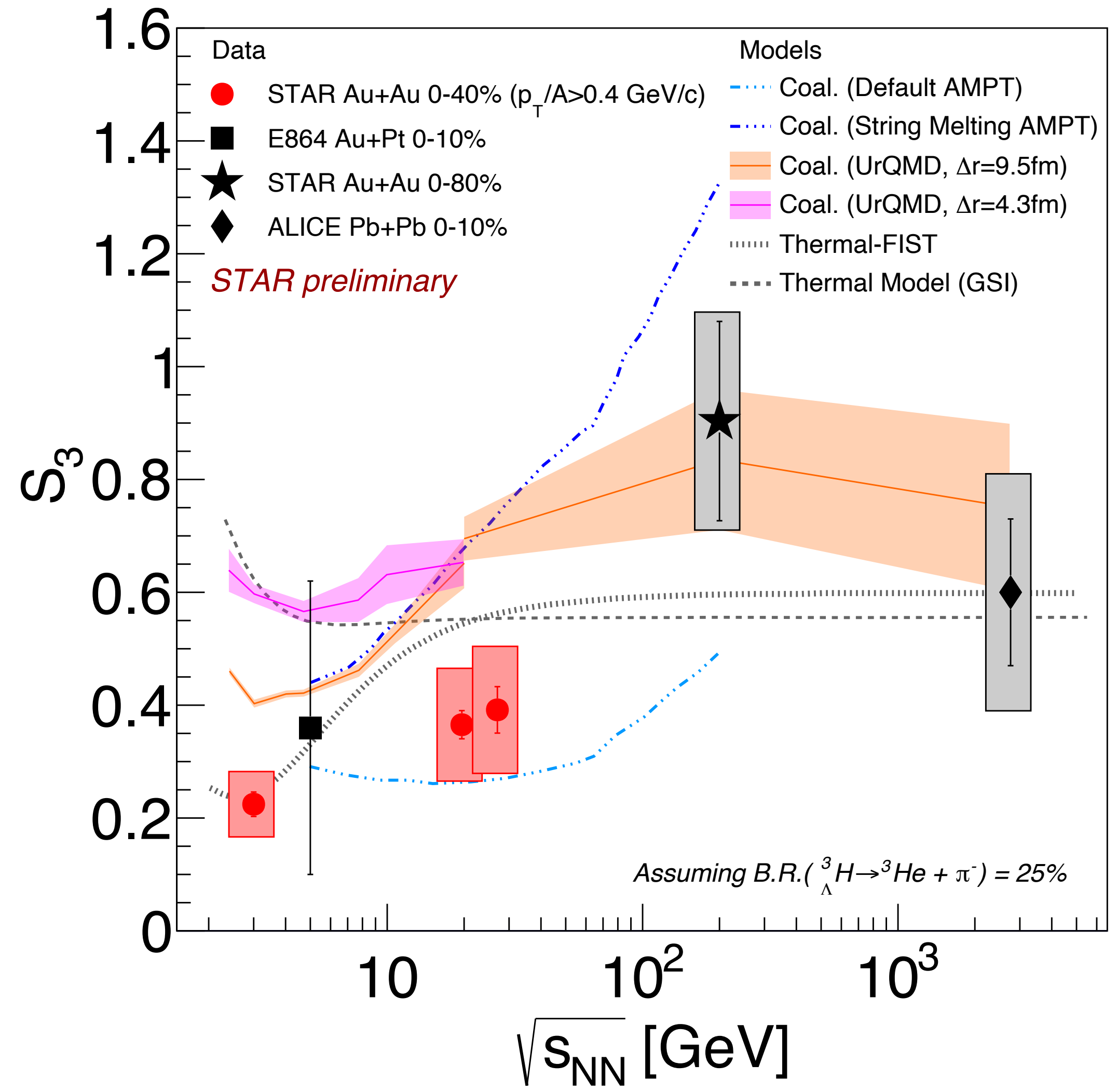
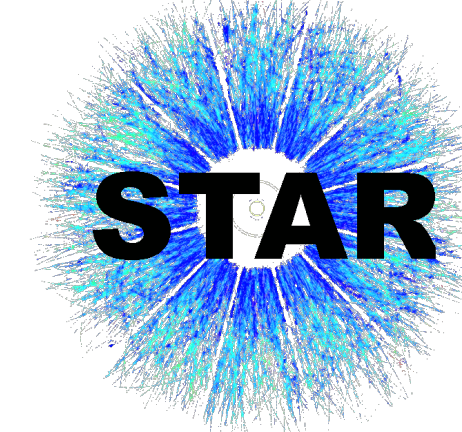
$S_4 > S_3 \rightarrow$ enhanced ${}^4_\Lambda \text{H}$ production due to feed-down from excited state



No obvious kinematic and centrality dependence of S_A is observed at 3 GeV.

\rightarrow Coalescence parameter B_A of $\Lambda^A \text{H}$ and $\Lambda^A \text{He}$ follows similar tendency versus p_T , rapidity and centrality.

Energy dependence of S_3



STAR, Science 328 (2010) 58

ALICE, PLB 754 (2016) 360

E864, PRC 70 (2004) 024902

NA49, J.Phys.Conf.Ser.110(2008)032010

A. Andronic et al, PLB 697 (2011) 203 (Thermal (GSI))

S. Zhang, PLB 684(2010)224 (Coal.+AMPT)

T. Reichert, J. Steinheimer et al, arXiv:2210.11876(2022) (UrQMD, Thermal-FIST)

- Data shows a hint of an increasing trend from $\sqrt{s_{NN}} = 3.0$ GeV to 2.76 TeV
- For coalescence models, the energy dependence is sensitive to the source radius (Δr)
- Thermal-FIST describes the S_3 data reasonably well

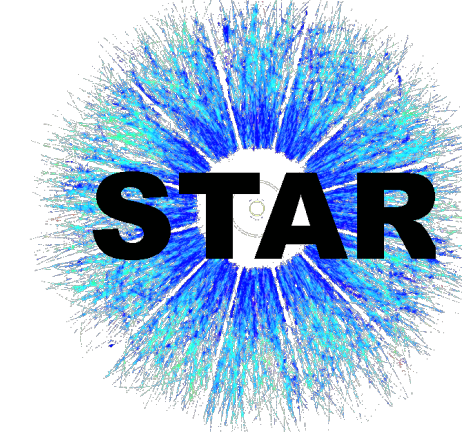
Summary



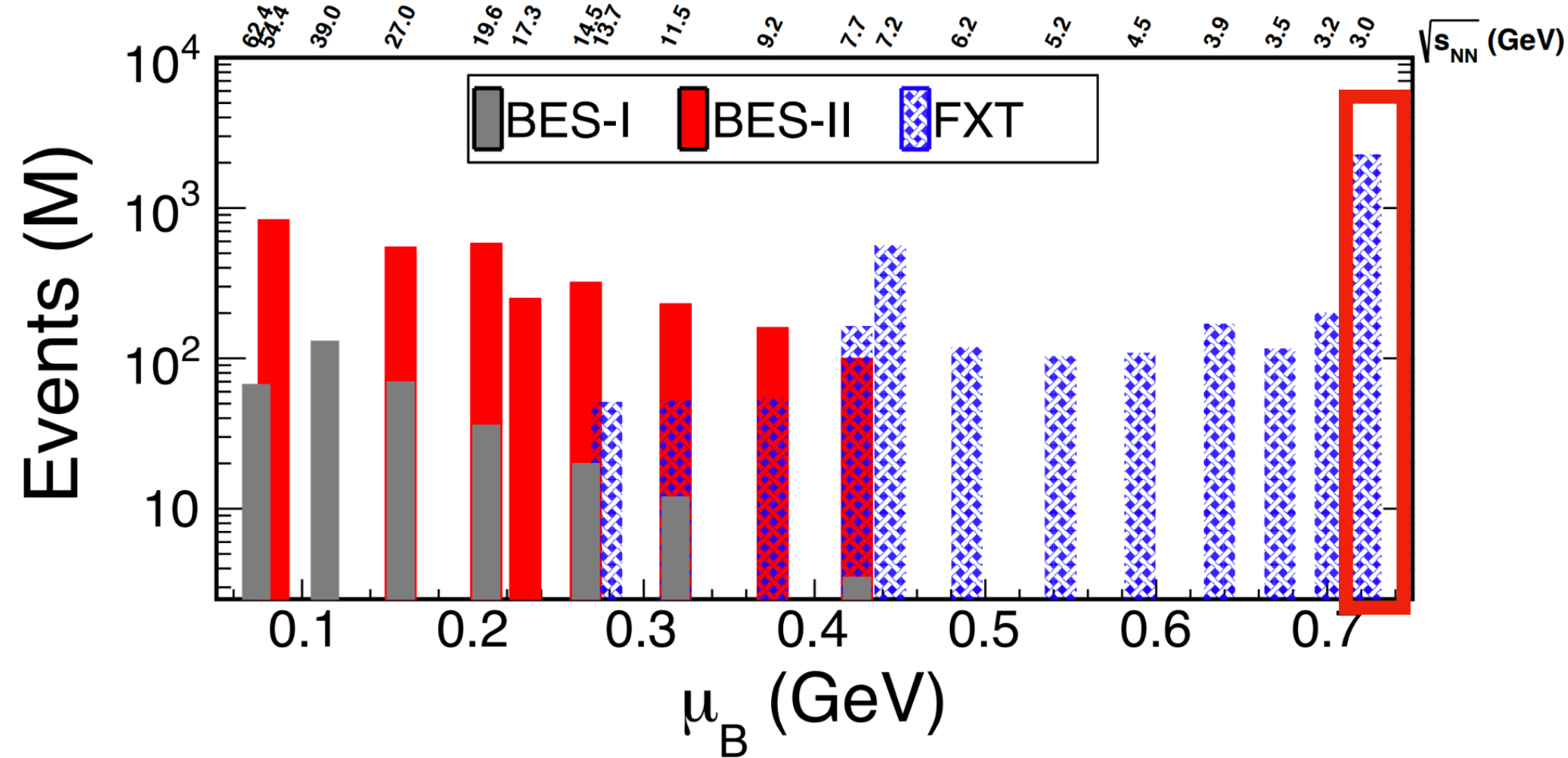
Presented measurements on hypernuclei production in the high-baryon-density region with high statistical precision using STAR data

- **Hypernuclei structure**
 - ${}^3_{\Lambda}\text{H}$, ${}^4_{\Lambda}\text{H}$ lifetimes and R_3 of ${}^3_{\Lambda}\text{H}$ measured with improved precision
 - Strong constraints on hyperon-nucleon interaction models
- **Hypernuclei production in heavy-ion collisions**
 - ${}^3_{\Lambda}\text{H}$, ${}^4_{\Lambda}\text{H}$ production yields at 3.0, 19.6 and 27 GeV
 - Coalescence models approximately describe the trends of ${}^4_{\Lambda}\text{H}$ rapidity distribution
 - S_3 and S_4 show weak centrality/kinematic dependence
 - Energy dependence of ${}^3_{\Lambda}\text{H}$, ${}^4_{\Lambda}\text{H}$ yields and S_3 compared with models are shown
 - Provide constraints to hypernuclei production models
 - ${}^3_{\Lambda}\text{H}$ and ${}^4_{\Lambda}\text{H}$ collectivity v_1
 - v_1 slopes follow mass number scaling -> Support coalescence picture

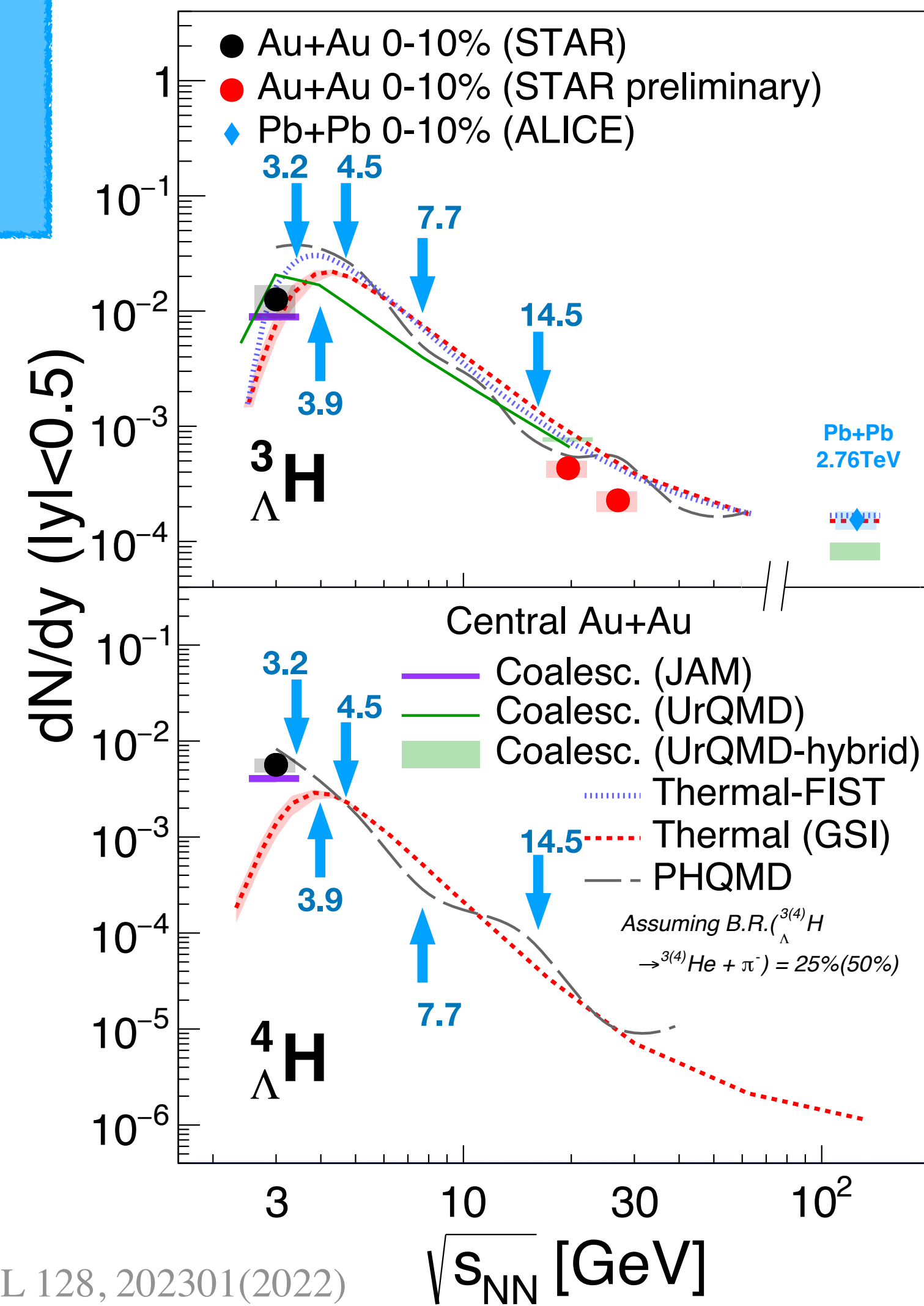
Outlook



1. iTPC and eToF fully installed in 2019 → improve η acceptance and PID at large η
2. High statistics data in STAR BES-II $\sqrt{s_{NN}} = 3.0 - 54.4$ GeV, especially the **2 billion events** collected at 3 GeV in 2021 → larger statistics, higher precision

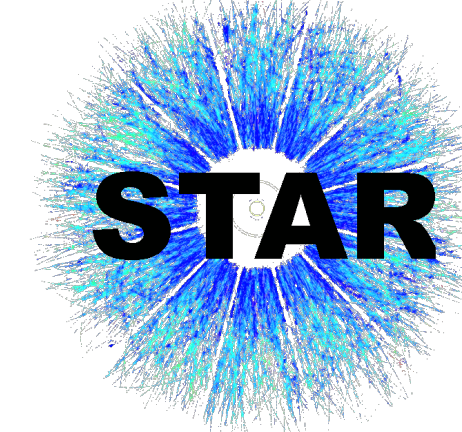


- Precision measurements on hypernuclei properties
- Energy dependence study of hypernuclei yields
- Search for double Λ hypernuclei
 - e.g. ${}^4_{\Lambda\Lambda}\text{He} \rightarrow {}^4_{\Lambda}\text{He}\pi$, ${}^5_{\Lambda\Lambda}\text{He} \rightarrow {}^5_{\Lambda}\text{He}\pi$

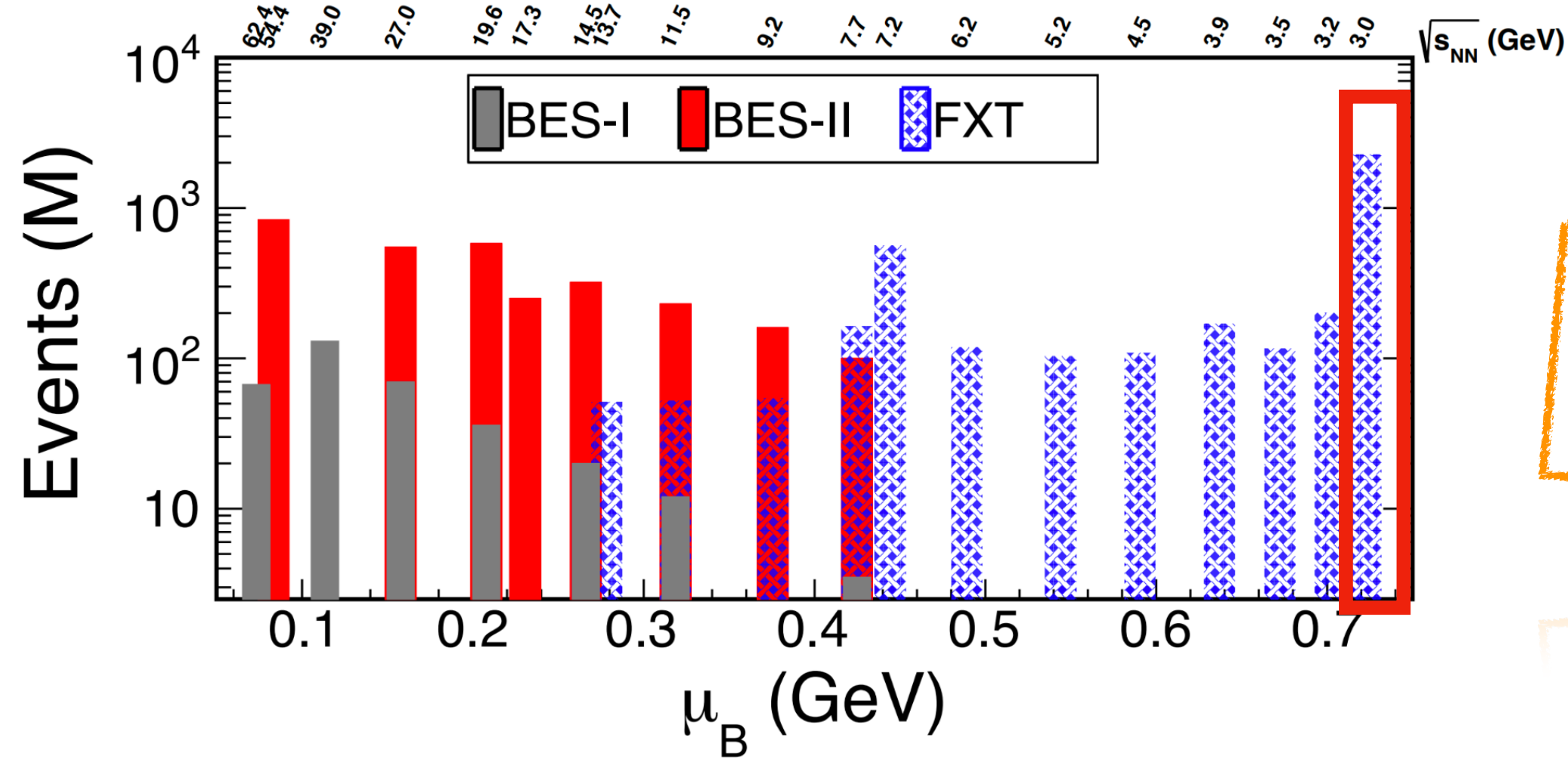


STAR, PRL 128, 202301(2022)

Outlook

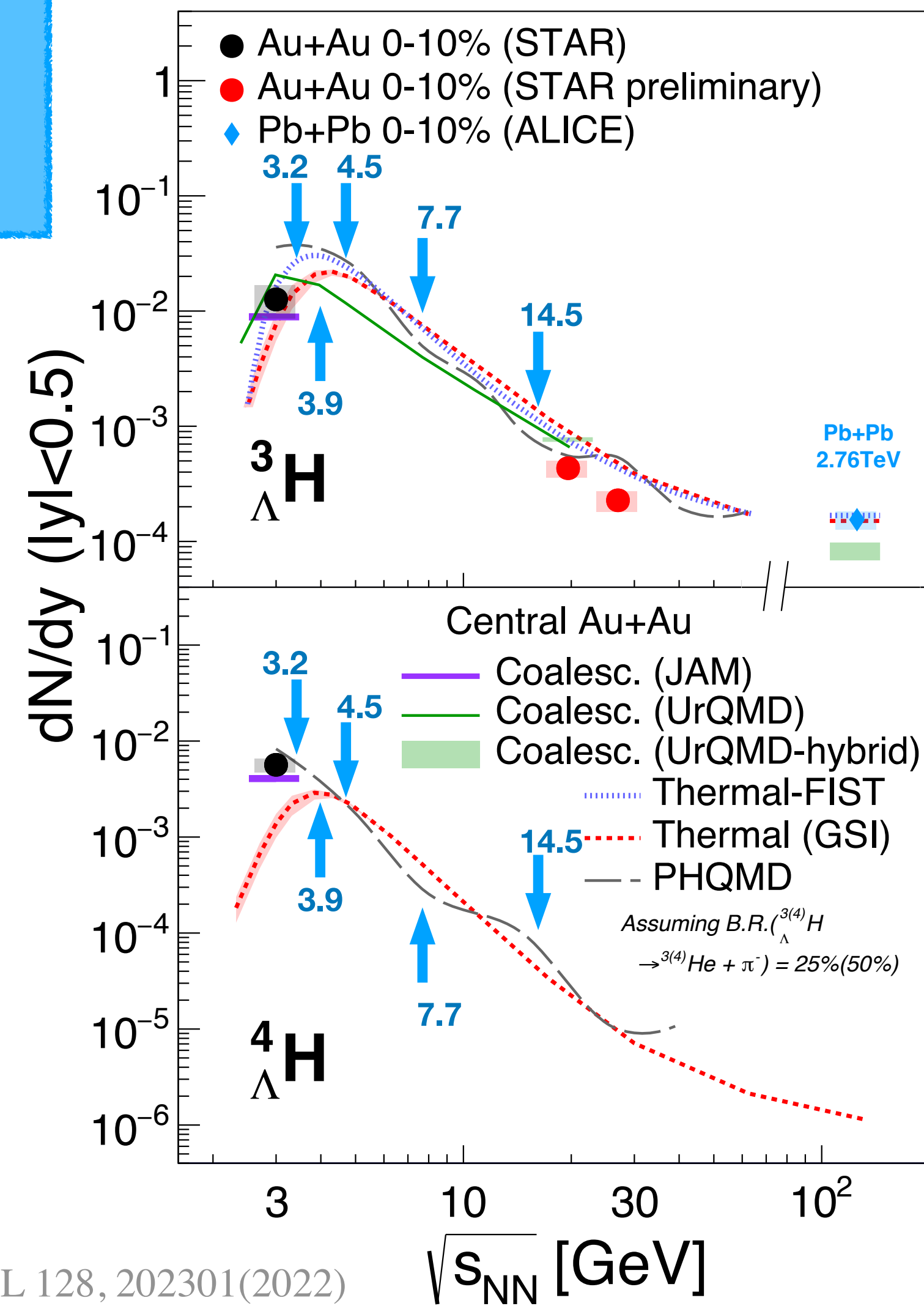


1. iTPC and eToF fully installed in 2019 → improve η acceptance and PID at large η
2. High statistics data in STAR BES-II $\sqrt{s_{NN}} = 3.0 - 54.4$ GeV, especially the **2 billion events** collected at 3 GeV in 2021 → larger statistics, higher precision



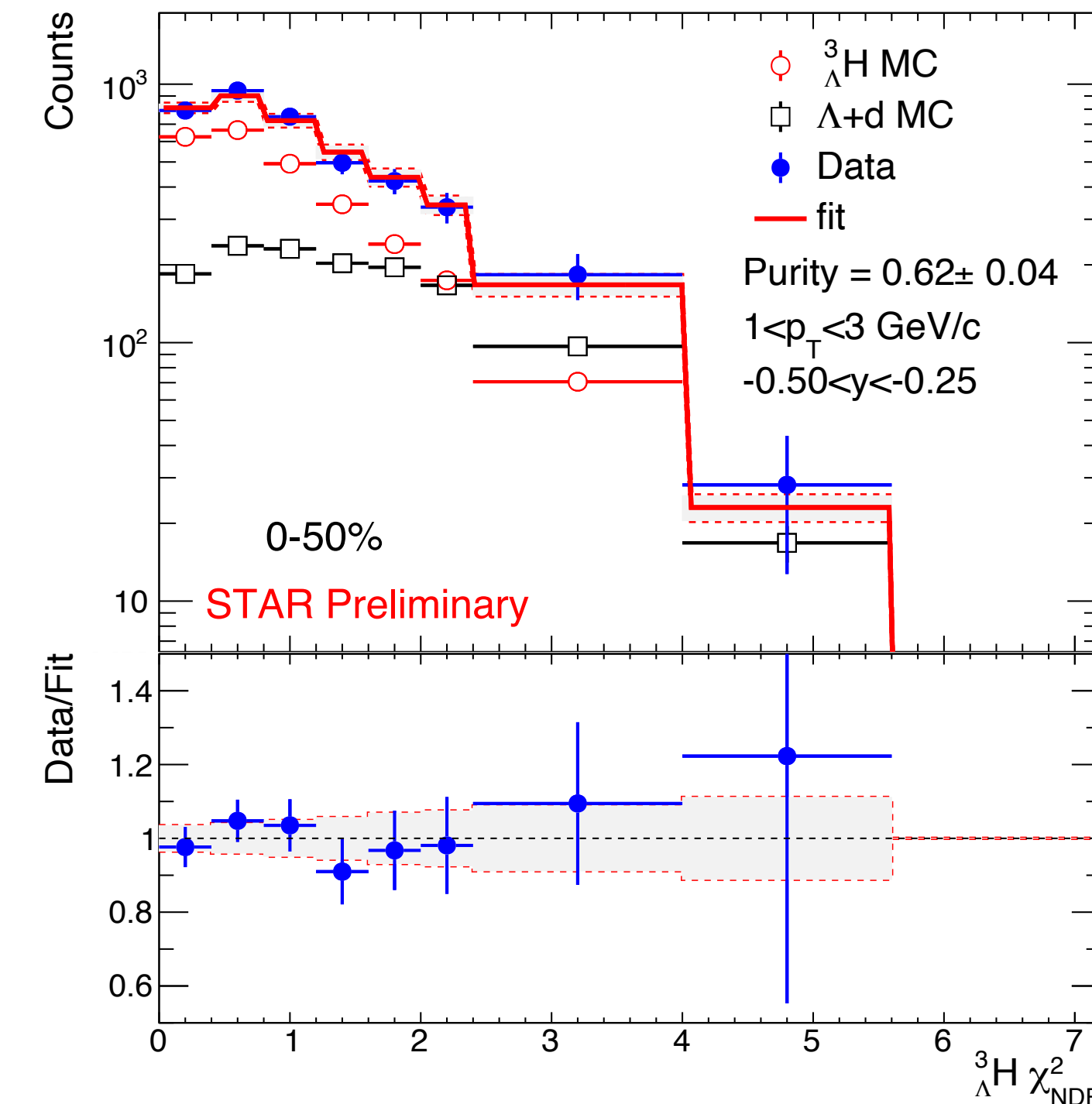
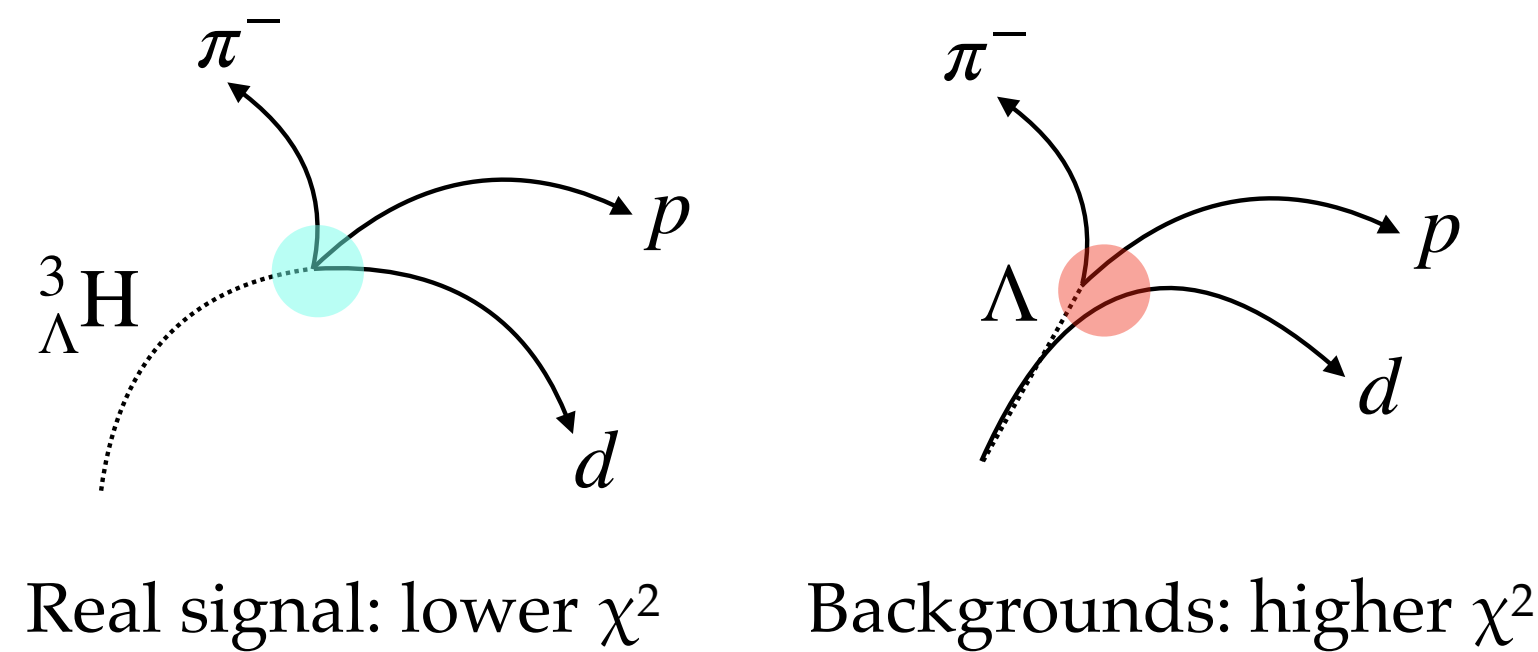
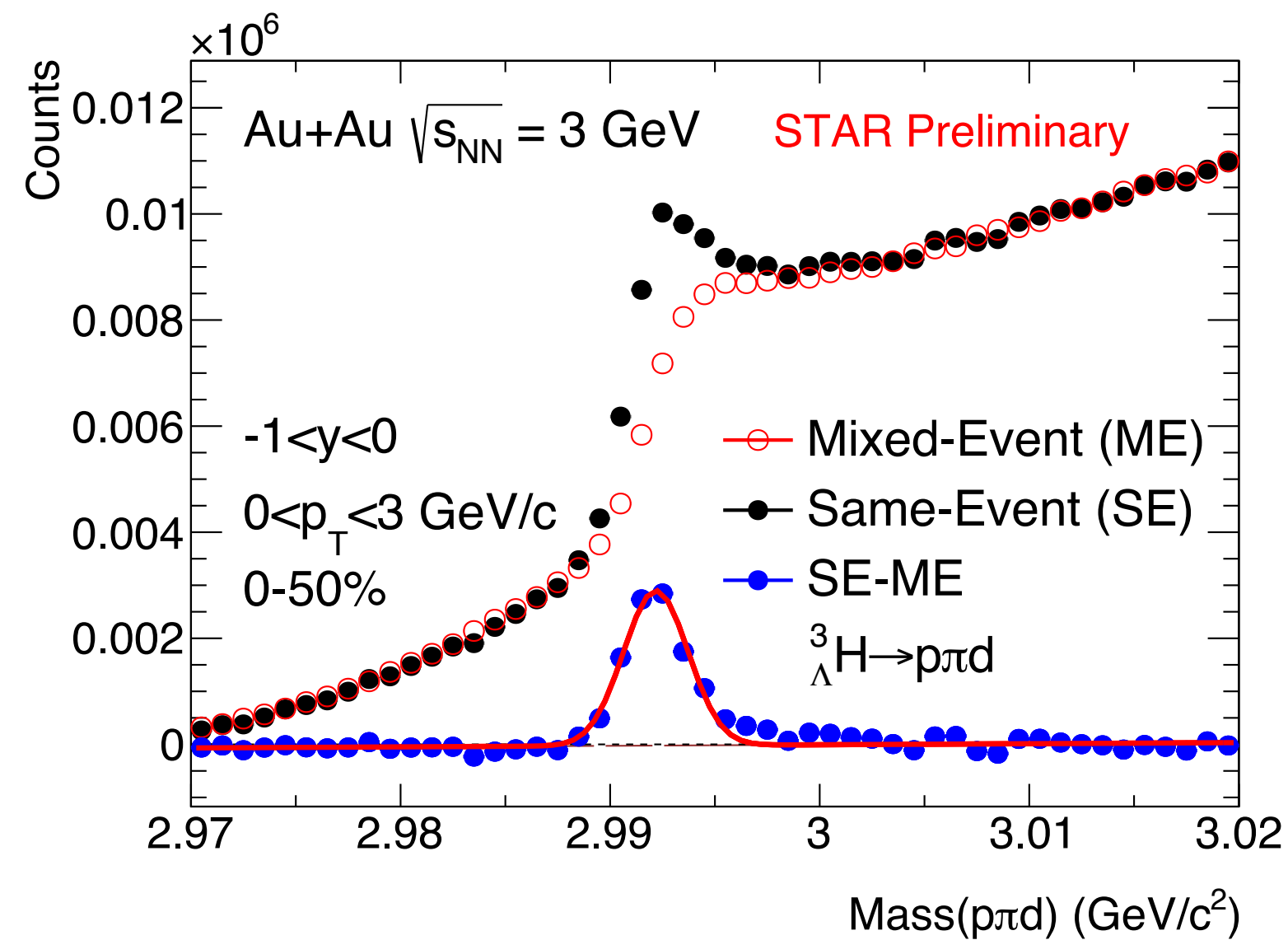
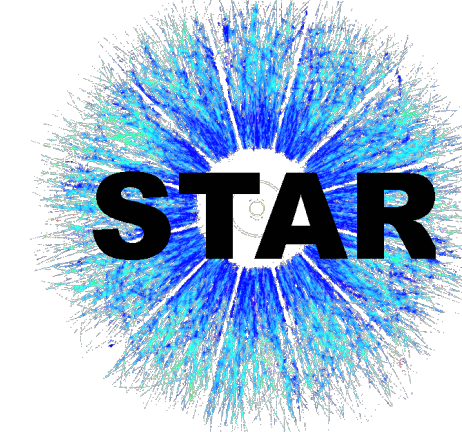
Thank you!

- Precision measurements on hypernuclei properties
- Energy dependence study of hypernuclei yields
- Search for double Λ hypernuclei
 - e.g. ${}^4_{\Lambda\Lambda}\text{He} \rightarrow {}^4_{\Lambda}\text{He}\pi$, ${}^5_{\Lambda\Lambda}\text{He} \rightarrow {}^5_{\Lambda}\text{He}\pi$



Backup slides

${}^3_{\Lambda}\text{H}$ 3-body signal



- SE-ME signals contains real signal and kinematically correlated $\Lambda + d(\Lambda \rightarrow p\pi^-)$

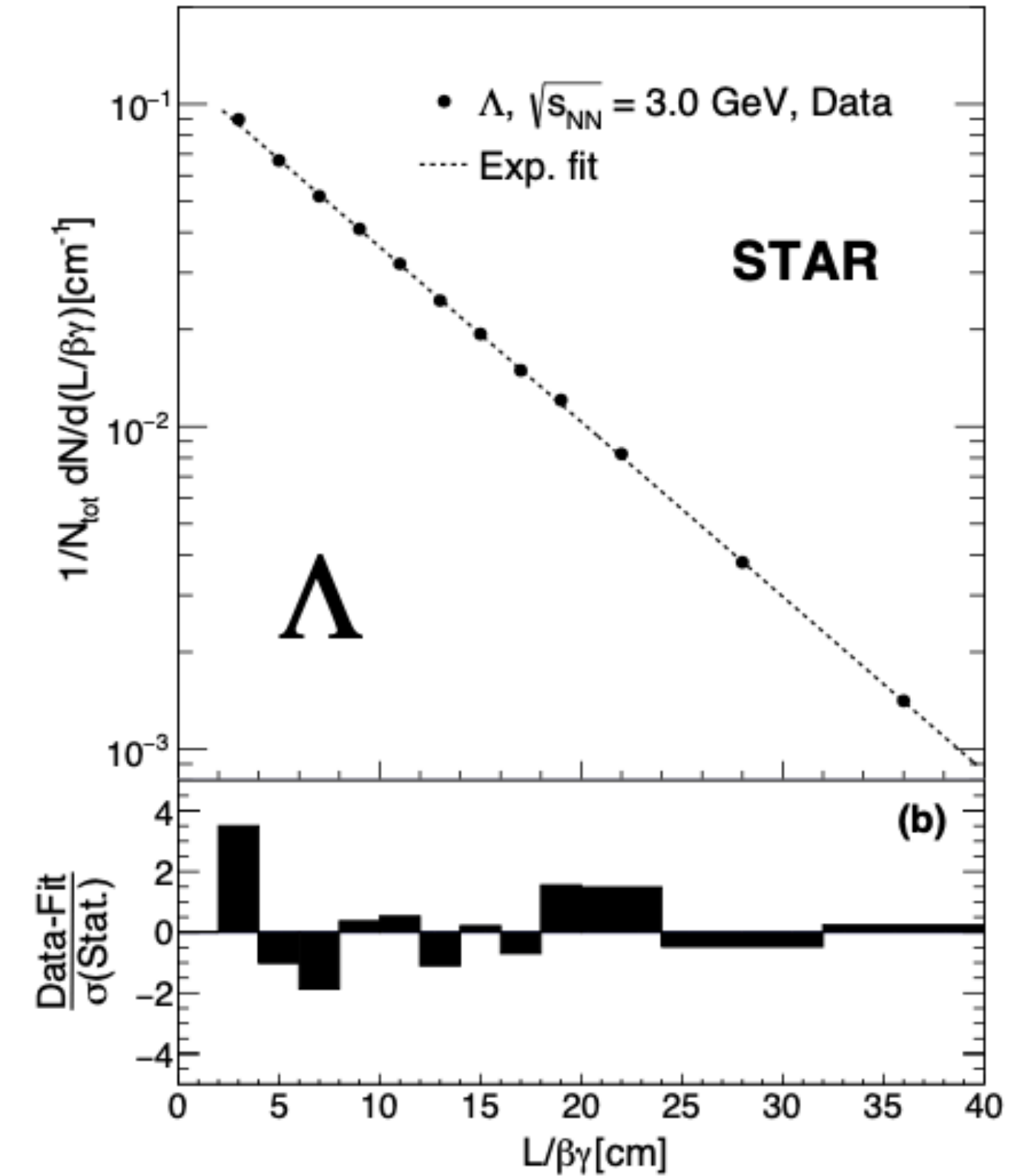
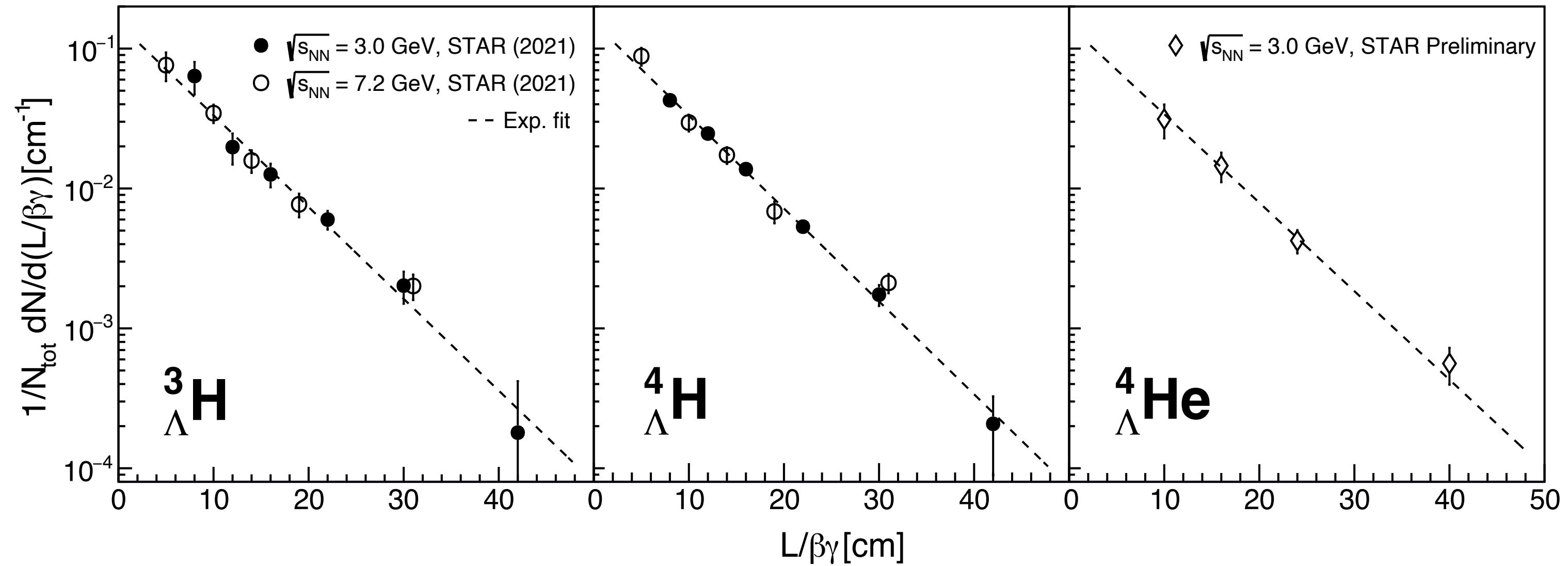
- Estimation of ${}^3_{\Lambda}\text{H}$ purity in signals

- Normalized χ^2_{NDF} distribution of $\Lambda + d$ and ${}^3_{\Lambda}\text{H}$ template from MC ($f_{\Lambda d}$ and $f_{{}^3_{\Lambda}\text{H}}$), and reconstructed signal f_{Data}

- Purity: the fraction of real ${}^3_{\Lambda}\text{H}$ signals $f_{{}^3_{\Lambda}\text{H}}$ in signals f_{Data} from fitting

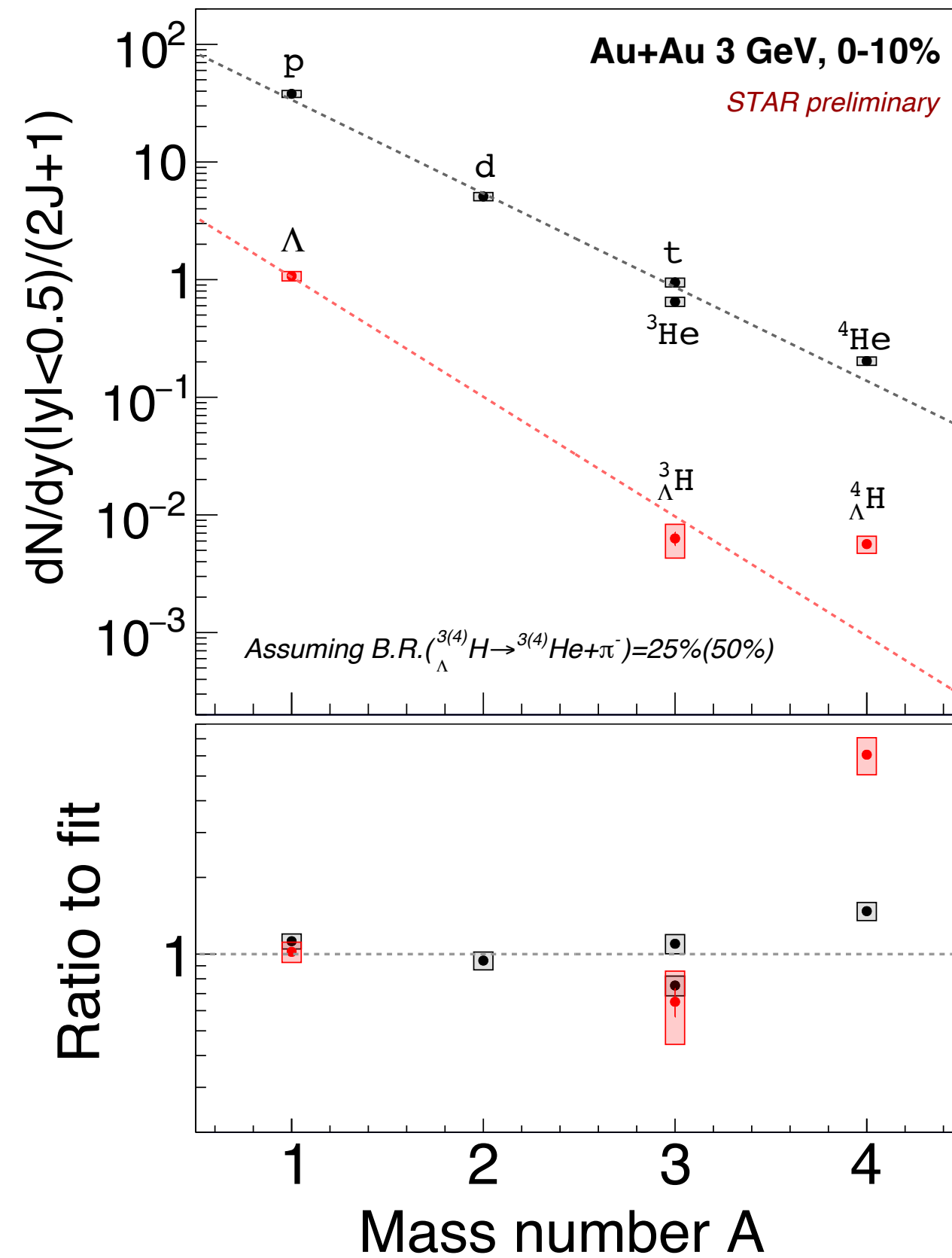
$$f_{Data} = p_0 \cdot (f_{\Lambda d} + p_1 \cdot f_{{}^3_{\Lambda}\text{H}})$$

Lifetime

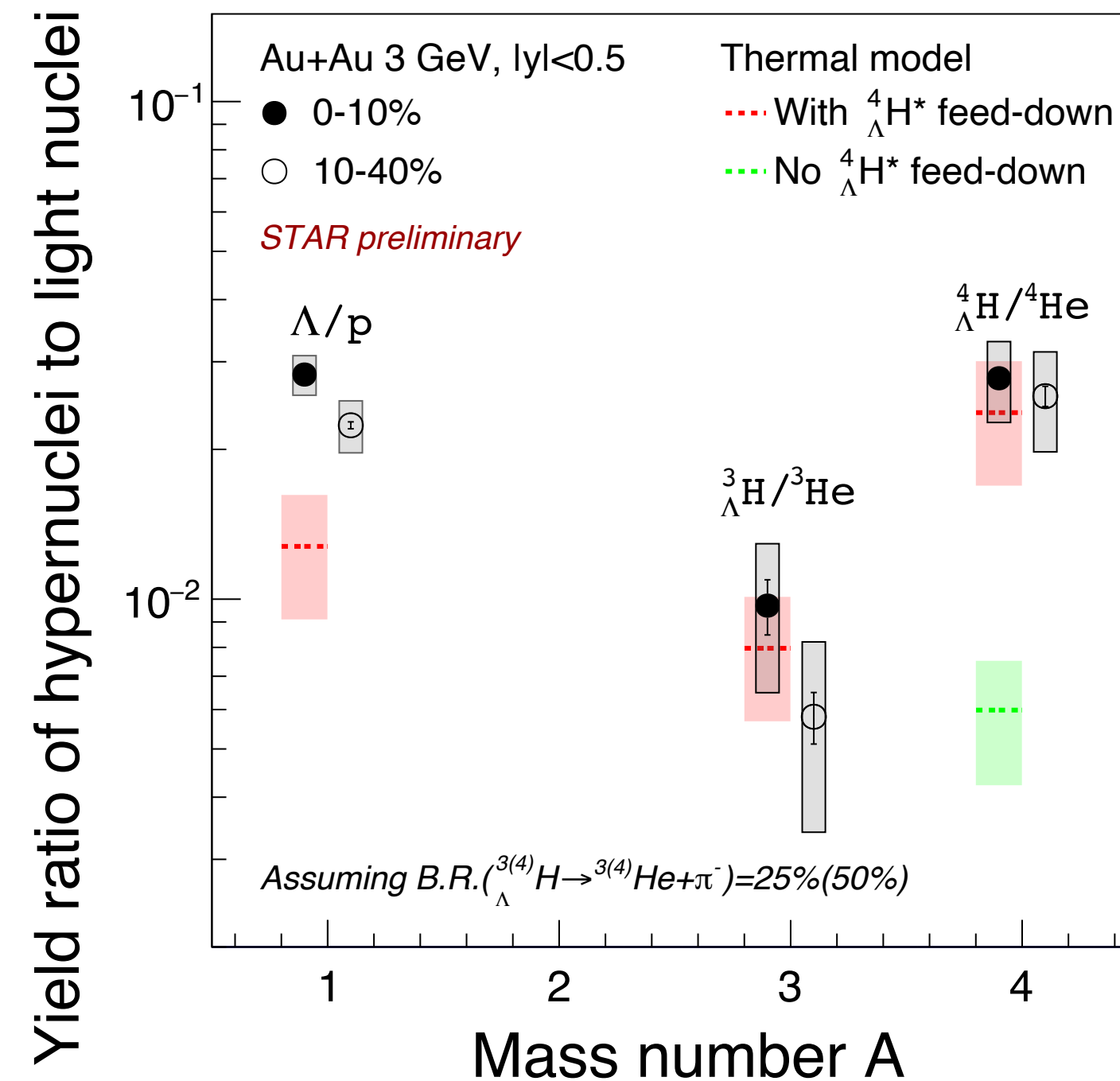


- Lifetime τ extracted via $N(t) = N_0 e^{-L/\beta\gamma c\tau}$
- Λ lifetime cross check : 267 ± 4 ps, consistent with PDG value (263 ± 2 ps)
- ${}^3_{\Lambda}\text{H}$ and ${}^4_{\Lambda}\text{H}$ lifetimes from 3.0 GeV consistent with 7.2 GeV results

Hyper-to-light nuclei ratios



- Thermal/coalescence models predict approx. exponential dependence of yields/(2J+1) vs A
- ${}^4_\Lambda\text{H}$ lies a factor of 6 above exponential fit to (Λ , ${}^3_\Lambda\text{H}$, ${}^4_\Lambda\text{H}$)



- Non-mononic behavior in light-to-hyper-nuclei ratio vs A observed
 - Thermal model calculations including excited ${}^4_\Lambda\text{H}^*$ feed-down shows a similar trend

A. Andronic et al, PLB 697 (2011) 203 (Thermal model)

- Non-existence of bound ${}^3_\Lambda\text{H}^*$ ($J^+ = 3/2$)
 - Data support creation of unstable A = 4 hypernuclei from heavy-ion collisions